

# Constraining the Barbero-Immirzi parameter from the duration of inflation in Loop Quantum Cosmology

L. N. Barboza,<sup>1,\*</sup> G. L. L. W. Levy,<sup>2,†</sup> L. L. Graef,<sup>1,‡</sup> and Rudnei O. Ramos<sup>2,§</sup>

<sup>1</sup>*Instituto de Física, Universidade Federal Fluminense,*

*Avenida General Milton Tavares de Souza s/n, Gragoatá, 24210-346 Niterói, Rio de Janeiro, Brazil*

<sup>2</sup>*Departamento de Física Teórica, Universidade do Estado do Rio de Janeiro, 20550-013 Rio de Janeiro, RJ, Brazil*

We revisit the predictions for the duration of the inflationary phase after the bounce in Loop Quantum Cosmology. We present our analysis for different classes of inflationary potentials that include the monomial power-law chaotic type of potentials, the Starobinsky and the Higgs-like symmetry breaking potential with different values for the vacuum expectation value. Our set up can easily be extended to other forms of primordial potentials than the ones we have considered. Independently on the details of the contracting phase, if the dynamics starts sufficiently in the far past, the kinetic energy will come to dominate at the bounce, uniquely determining the amplitude of the inflaton at this moment. This will be the initial condition for the further evolution that will provide us with results for the number of  $e$ -folds from the bounce to the beginning of the accelerated inflationary regime and the subsequent duration of inflation. We also discuss under which conditions each model considered could lead to observable signatures on the spectrum of the Cosmic Microwave Background (CMB), or, else, be excluded for not predicting a sufficient amount of accelerated expansion. A first analysis is performed considering the standard value for the Barbero-Immirzi parameter,  $\gamma \simeq 0.2375$ , which is obtained from black hole entropy calculations. In a second analysis, we consider the possibility of varying the value of this parameter, which is motivated by the fact that the Barbero-Immirzi parameter can be considered a free parameter of the underlying quantum theory in the context of Loop Quantum Gravity. From this analysis, we obtain a lower limit for this parameter by requiring the minimum amount of inflationary expansion that makes the model consistent with the CMB observations.

## I. INTRODUCTION

Inflation, which is the current paradigm for the early Universe cosmology, has been extremely successful from a phenomenological point of view. It predicted the spatial flatness of the Universe, the homogeneity seen in the Cosmic Microwave Background (CMB), besides suggesting a causal explanation for the origin of its anisotropies, providing the first theory for the origin of the large-scale structure of the Universe based on fundamental physics. Although requiring a certain amount of fine-tuning on its constants [1–3] the inflationary scenario predicts correctly the primordial power spectra, whose evolution determine the temperature fluctuations in the CMB and the formation of the large-scale structure of the Universe [2, 4], having been developed before most of the data we now have was in hand.

However, despite the success of inflation, in the classical theory of general relativity (GR), all scalar field models of inflation experience the big bang singularity that is inevitable [5, 6]. The singularity problem is the result of an extrapolation of GR beyond the limits where the theory is well justified. This implies in additional difficulties in the definition of initial conditions due to the absence of a regular surface where those initial con-

ditions can be established. Another related problem in the context of inflation in GR is the fact that there is a very limited value for the number of inflationary  $e$ -folds which makes the model theoretically consistent. We know that in order to be compatible with observations, the number of  $e$ -folds during inflation should be at least 60 or so. Meanwhile, in some cases, the predicted number of  $e$ -folds is more than 70 [7]. In those cases, the scale of the fluctuations which are today observed in the CMB was smaller than the Planck length at the starting of inflation. As a result, the usual semiclassical treatment during inflation are questionable, which is known as the trans-Planckian problem [8, 9]. These issues with the consistency of inflation also motivate to consider scenarios with a well-defined pre-inflationary dynamics, free of singularities [10–12]. In these scenarios, cosmological perturbations will reach the beginning of inflation in a quantum state excited relative to the Bunch-Davis vacuum, affecting the power-spectra, thus potentially leaving marks on the CMB [13]. In order to address these important issues, one must consider a scenario of quantum gravity acting in the high energy regime. The scenario we consider here lies in the context of *Loop Quantum Gravity* (LQG).

LQG proposes a quantization formalism based on a nonperturbative and background-independent formulation of the geometric degrees of freedom [14–20]. In its canonical formulation, it is aimed to respect the general covariance of Einstein’s theory. In particular, in GR the Hamiltonian is a linear combination of constraints which, via Poisson brackets, generates diffeomorphism transfor-

---

\* lauziene.barboza@gmail.com

† guslevy9@hotmail.com

‡ leilagraef@id.uff.br

§ rudnei@uerj.br

mations, the fundamental symmetry of the theory [21]. LQG, on the other hand, adopts the quantization scheme proposed by Dirac for systems with constraints, which consists in requiring that those constraints are satisfied at the quantum level on the physical states of the system. The geometric degrees of freedom are described in LQG by pairs of canonical variables, the Ashtekar variables, that consist of the components of a densitized triad and a gauge connection. The quantization is obtained through holonomies of the connections and fluxes of the densitized triads.

Loop Quantum Cosmology (LQC) is the symmetry reduced version of LQG [18], applied to cosmological models [16, 17, 22]. Taking into account such quantum geometric effects described by LQG in cosmological scenarios, Einstein's equations maintain an excellent degree of approximation in the low curvature regime. However, in the Planck regime they undergo major changes, driving a non-singular bounce due to repulsive quantum geometry effects [14, 20], then naturally solving the big bang singularity problem. Therefore, in the LQC framework, for matter satisfying the usual energy conditions, whenever a curvature invariant grows near the Planck scale in LQC, the effects of quantum geometry dilute it [14].

In LQC models with a kinetic energy dominated bounce, as the ones we are going to consider, an inflationary phase almost inevitably follows the bounce phase (see, e.g., Refs. [10, 11, 23–26]). The duration of this inflationary phase is quantified by the number of  $e$ -folds [27–30]. As it is well known [31], the inflationary phase must last at least around 60  $e$ -folds or so in order to solve the problems of the standard cosmological model. However, in LQC, as shown in Ref. [32], the bounce and pre-inflationary dynamics leaves imprints on the spectrum of the CMB. In Ref. [10] it was shown that, in order to be consistent with observations, the Universe in LQC must have expanded at least around 141  $e$ -folds from the bounce until today. This is so because LQC can lead to scale-dependent features in the CMB spectrum, and the fact that we do not observe them today means that they must have been well diluted by the post-bounce expansion of the Universe. This implies an extra number of inflationary  $e$ -folds in LQC, given by  $\delta N \sim 21$  [10]. On the other hand, if the number of extra inflationary  $e$ -folds is much higher than this value the features imprinted in the CMB spectrum due to the LQC effects would be overly diluted and, in this case, LQC cannot be directly tested even by forthcoming experiments.

Such theoretical results motivate an investigation of the number of  $e$ -folds in models of LQC. This can be performed consistently with initial conditions defined either in the bounce, as done, e.g., in Refs. [10, 33], or in a contraction phase before the bounce, as considered in Refs. [34–37], for example. In particular, with the authors of the latter references claiming that taking initial conditions in the far past in the contracting phase should be the appropriate approach to study the probability of inflation after the bounce. Both approaches for choos-

ing the initial conditions to investigate the probability of inflation in LQC were applied to many different potentials. For instance, power-law potentials were considered in Refs. [11, 30, 34–38], alpha-attractor potentials in Ref. [26], monodromy potentials with a modulation term in Ref. [24] and also chaotic and Starobinsky potentials in the framework of standard and modified LQC models [25]. In particular, in the work of Refs. [29, 30], in addition of considering different classes of potentials, the effect of radiation as an additional ingredient of the energy density budget around the bounce has been considered, showing that the duration of inflation is dependent not only on the inflaton potential but also on the amount of radiation in the Universe prior to the start of the inflationary regime.

In the present paper, we show that there are well defined values for the inflaton amplitude at the bounce, which can be estimated analytically and depending only on the form of the primordial inflaton potential. Then, we provide explicit results, also analytically, for the duration of the pre-inflationary phase and for the inflaton amplitude at the beginning of the inflationary regime. This then allows us to explicitly obtain the total number of  $e$ -folds that inflation will have. Our results are sufficiently general such that it can easily be extended to many different forms of the primordial inflaton potential other than the ones we have focused in this paper.

In the analysis we consider in the first part of this paper, we consider the standard value for the *Barbero-Immirzi parameter*,  $\gamma$ , which is the one arising from the calculation of the entropy of black holes [39]. But then in the second part, we will consider the Barbero-Immirzi parameter as a free variable of the theory. This is motivated by the fact that the role of the Barbero-Immirzi parameter has been a topic of much discussion in the literature (see, e.g., Refs. [40–49]). Often, the recovering of the Bekenstein-Hawking entropy has been considered as a way to fix its value, however, the strong dependence of the entropy calculation on  $\gamma$  is controversial. The semiclassical thermodynamical properties can actually be recovered for any value of  $\gamma$  if one makes the appropriated assumptions. It is, after all, a coupling constant with a topological term in the action of gravity, with no consequence on the classical equations of motion. What is known is that the appearance of this parameter in the area and volume spectra implies that it plays a role in determining the fundamental length scale of space. Such emergence occurs as a rescaling of lengths, motivating a possible interpretation according to Ref. [50]. When introducing the notion of the horizon into quantum theory, it was concluded that the entropy of large black holes is independent of this parameter and, as it was believed, it is only quantum gravity corrections to the entropy and temperature of small black holes that depend on the Barbero-Immirzi parameter. Therefore, since  $\gamma$  is a free parameter of the theory, its important to find ways to constraint its value, especially from observations if possible. If one could resolve distances of around the Planck

length, one would be able to fix the Barbero-Immirzi parameter via experiment. Once again, cosmology seems to be a window of opportunity to access such scales, which are unreachable by any terrestrial experiments. As previously discussed, the quantum bounce changes the scalar power spectrum by a correction term which depends on the characteristic scale at the bounce. The characteristic scale is the shortest scale (or largest wavenumber, namely  $k_B$ ) that feels the spacetime curvature during the bounce. As this characteristic scale is dependent on the Barbero-Immirzi parameter, we have an unique opportunity to constrain  $\gamma$  through the observational constraints put on  $k_B$  itself.

In previous works (see for instance Refs. [10, 51]), precise constraints on the correction term in the power spectrum of LQC was obtained using the recent CMB data. This observational analysis provided constraints on the characteristic scale  $k_B$ . This scale is a function of the Barbero-Immirzi parameter and of the number of  $e$ -folds of expansion from the bounce until today. The suggestion of considering the Barbero-Immirzi parameter as a free quantity was in fact first considered in Ref. [34]. In the present paper, we, however, push that idea much further by taking advantage of our analysis and results obtained in the first part of this paper. Then, by using the observational constraints on  $k_B$ , we also study their dependence on the Barbero-Immirzi parameter. This will allow us to impose some precise limits on the value of  $\gamma$  as a function of the  $e$ -folding number (or equivalently, to obtain constraints on the  $e$ -fold number as a function of  $\gamma$ ) depending on the primordial inflaton potential.

In summary, in this paper we keep investigating the intriguing possibility that the quantum regime of the Universe in the context of LQC could leave observable signals on CMB, going beyond earlier works in at least two important aspects: (a) Firstly, we investigate the duration of inflation for different potentials including the Starobinsky and Higgs-like potential in addition to the monomial ones, considering that the initial conditions are uniquely determined at the bounce and once we trace the dynamics far back in the contracting phase. However, our methods are general enough to be able to be extended to other forms of primordial potentials. For practical purposes, we obtain the quantities at some point in the contracting phase and where the kinetic energy of the inflaton starts to dominate over that from the potential. From that point on, we can forward the evolution up to the end of the accelerated inflationary regime; (b) Secondly, we consider the *Barbero-Immirzi parameter* as a free variable of the theory. From our analysis, we then obtain, for the first time, a lower limit for this parameter by requiring the model to be consistent with the CMB observations.

This paper is organized as follows. In Sec. II, we briefly present the main equations of LQC, and also introduce the potentials that we are going to consider in our analysis. In Sec. IIIB, we describe the method used in our analysis and we also establish the way that the initial con-

ditions can be determined and that we are going to use in obtaining the subsequent background dynamical evolution up to the end of inflation. In Sec. IV, we present the results obtained for the duration of inflation in each model considered. The analytical results obtained here are also compared with the numerical results obtained from previous statistical analysis derived in Ref. [30] and in other references. In Sec. V, we discuss the constraints on the value of the Barbero-Immirzi parameter from the required number of inflationary  $e$ -folds in each model. In Sec. VI we give our conclusions. One appendix is included to show some technical details.

## II. THEORETICAL BASIS

In this section we briefly introduce the main equations of LQC and we also present the models we are going to consider in this paper.

As discussed in Ref. [33], in LQC the spatial geometry is described by the variable  $\nu$  proportional to the physical volume of a fiducial cubical cell, in place of the scale factor  $a$ , i.e.,

$$\nu = -\frac{\mathcal{V}_0 a^3 m_{\text{Pl}}^2}{2\pi\gamma}, \quad (2.1)$$

where  $\mathcal{V}_0$  is the comoving volume of the fiducial cell,  $m_{\text{Pl}} \equiv 1/\sqrt{G} = 1.22 \times 10^{19}$  GeV is the Planck mass, with  $G$  the Newton's gravitational constant and  $\gamma$  is the Barbero-Immirzi parameter. Although  $\gamma$  is actually a free parameter of the theory, in the first part of our work we are going to consider the value motivated from the calculation of the black hole entropy in LQG, which is  $\gamma \simeq 0.2375$  [52] and that is also the value considered in most of the studies in LQC.

The Friedmann equation in LQC assumes the form [33]

$$\frac{1}{9} \left( \frac{\dot{\nu}}{\nu} \right)^2 \equiv H^2 = \frac{8\pi}{3m_{\text{Pl}}^2} \rho \left( 1 - \frac{\rho}{\rho_{cr}} \right), \quad (2.2)$$

where

$$\rho_{cr} = \frac{\sqrt{3}m_{\text{Pl}}^4}{32\pi^2\gamma^3}, \quad (2.3)$$

is the critical density. Through the modified Friedmann equation (2.2), we see explicitly the underlying quantum geometric effects [14], leading to a bounce in replacement of the singularity when  $\rho = \rho_{cr}$ . For  $\rho \ll \rho_{cr}$  we recover GR as expected.

The energy density  $\rho$  in the Eq. (2.2) respects the usual conservation equation,

$$\dot{\rho} + 3H(\rho + p) = 0, \quad (2.4)$$

where  $p$  is the pressure density.

In models of a single scalar field  $\phi$  with a potential  $V(\phi)$ , in the Friedmann-Lemaître-Robertson-Walker

(FLRW) background, the effective equation of motion for  $\phi$ , the inflaton, is simply

$$\ddot{\phi} + 3H\dot{\phi} + V_{,\phi} = 0, \quad (2.5)$$

where  $V_{,\phi} \equiv dV(\phi)/d\phi$  is the derivative of the inflaton's potential.

In the following, we are going to present the models we are going to consider.

### A. Models

The classes of inflationary models we are going to consider are described by the potentials below.

#### 1. Power-law monomial potentials

In this class of models, the potential is given by

$$V = \frac{V_0}{2n} \left( \frac{\phi}{m_{\text{Pl}}} \right)^{2n}, \quad (2.6)$$

where  $n$  is some power. In this paper we will compare our results with available ones for the cases for the quadratic, quartic and sextic forms of the potential (corresponding to the powers  $n = 1, 2$  and  $3$ , respectively). The model given by Eq. (2.6) covers the class of inflationary models corresponding to large-field models [53].

The new data release from BICEP/Keck [54] strengthened the bounds on the tensor-to-scalar ratio  $r$ , putting severe constraints in the full class of monomial potentials, showing that they are disfavored in the context of standard inflation. However, these potentials, besides of being well motivated from a particle physics point of view, they can still be perfectly allowed in other frameworks, like in the context of warm inflation for example (see, e.g., Ref. [55] and references therein). Since our current analysis can be extended to such frameworks, we consider to be important to address this class of potentials here.

#### 2. The Higgs-like symmetry breaking potential

The Higgs-like symmetry breaking potential is given by the following expression,

$$V = \frac{V_0}{4m_{\text{Pl}}^4} (\phi^2 - v^2)^2, \quad (2.7)$$

where  $v$  denotes the vacuum expectation value (VEV) of the field. The Higgs-like symmetry breaking potential is another well motivated model from particle physics. Besides of that, it can represent either a small-field inflation model, if inflation starts (and ends) at the small field part of the potential (i.e., for  $|\phi| < |v|$ ), or be a large field model, if inflation happens in the large field region of the potential ( $|\phi| > |v|$ ). In all our analysis with this

potential, we have explicitly distinguished these two possibilities and produced results for both of them and by also considering different values for the VEV  $v$ .

#### 3. The Starobinsky potential

The Starobinsky model [56] is an example of a limiting case of more general modified gravity theories. When expressed in the Einstein frame, it represents a potential which can be written as

$$V = V_0 \left( 1 - e^{-\sqrt{\frac{16\pi}{3}} \frac{\phi}{m_{\text{Pl}}}} \right)^2. \quad (2.8)$$

The inflation results derived from the model Eq. (2.8) agree quite well with the observational data for the tensor-to-scalar ratio and spectral tilt [4]. For that reason, it is a popular form of potential in inflation studies.

Note that in Eqs. (2.6), (2.7) and (2.8), the scale  $V_0$  is fixed differently depending on the potential. Its value is determined by the amplitude of the CMB scalar spectrum. Details about its evaluation for the three forms of potentials considered here is giving in the Appendix A for completeness.

## III. BACKGROUND DYNAMICS IN LQC

The dynamics in the LQC models considered here is assumed to start in the contracting phase sufficiently before the bounce and as originally assumed to be the appropriate moment for setting the initial conditions [34]. Assuming that the initial conditions are set in the contracting phase, when the inflaton field is in the oscillating regime, then, considering a generic inflaton potential of the form  $V \propto \phi^m$ ,  $m > 0$ , it then follows that the inflaton field amplitude is expected to evolve as a function of the scale factor  $a(t)$  as [57]  $\phi \propto a(t)^{-6/(m+2)}$ . Thus, in the oscillating regime we have that  $V \propto a(t)^{-6m/(m+2)}$ , while the inflaton's kinetic energy will behave like  $\dot{\phi}^2 \propto a(t)^{-6}$ . Thus, for any finite value for the exponent  $m$ , with the oscillating phase lasting long enough in the contracting phase, the kinetic energy of the inflaton field will necessarily come to dominate at the bounce. As we are going to show in this section, with the kinetic energy dominating at the bounce, the value of the inflaton field,  $\phi_B$ , will then be uniquely determined at this moment. This result is independent on the details of the contracting phase, provided that the evolution starts sufficiently back in the contracting phase and in the oscillatory regime for the inflaton. The obtained value for  $\phi_B$  for each model provides the initial conditions for the further evolution of the system and which can be carried out up to the end of the accelerated inflationary regime.

In LQC models in which the evolution of the inflaton field is dominated by its kinetic energy at the quantum bounce, a slow-roll inflation phase is practically always

reached as demonstrated in many previous papers [10, 29, 30, 33, 34, 36]. Our goal here will be to estimate the number of  $e$ -folds of expansion in two regimes: In the pre-inflationary one, which includes the instant of the bounce till the beginning of slow-roll inflation. We denote this number of  $e$ -folds of expansion as  $N_{\text{pre}}$ . Then, the  $e$ -folds from the beginning to the end of inflation, which we call  $N_{\text{infl}}$ , is also determined. In order to achieve this, let us first begin by analyzing the background dynamics in our scenario starting from the bounce phase. We will proceed without assuming a specific model for the contracting phase.

Immediately before and after the bounce, assumed to happen at a time instant  $t_B$ , if the energy density is mostly dominated by kinetic energy as we are going to consider and discussed above, we have a phase of *superdeflation* (for  $t < t_B$ ) and *superinflation* (for  $t > t_B$ ). These are very short phases, which start close to the bounce instant (when  $H = 0$ , i.e.,  $\rho = \rho_{\text{cr}}$ ). They start (at  $t < t_B$ ) and ends (at  $t > t_B$ ) when  $\dot{H} = 0$ . The conditions for superdeflation/superinflation are

$$H^2 \gg |V_{,\phi}|, \quad \dot{\phi}^2/2 \gg V(\phi). \quad (3.1)$$

Right after the superinflation phase, in the post-bounce phase, the kinetic energy quickly decreases as  $\dot{\phi}^2 \propto 1/a^6$ , while the potential energy density  $V(\phi)$  only changes slowly. The inflaton dynamics after the bounce and throughout the pre-inflationary phase is just monotonic [10]. After a given moment, the potential energy of the inflaton will eventually dominate the energy content of the Universe and the standard slow-roll inflationary phase will set in. Before the beginning of slow-roll, the quantum corrections to the Friedmann equation are negligible, and the cosmological equations reduce to the usual ones of GR, at which point we then have that

$$\rho_{\text{cr}} \ll \rho, \quad V(\phi) \gg \dot{\phi}^2/2. \quad (3.2)$$

More specifically, the evolution of the Universe for  $t \geq t_B$  and prior to reheating (end of inflation) is divided into three different phases: *the bouncing*, *the transition* and *slow-roll inflation* [10]. Next, we describe each of these phases.

### A. Kinetic dominated regime

This phase is dominated by the kinetic energy of the inflaton, with  $\dot{\phi}^2/2 \gg V(\phi)$ . In Eq. (2.5), neglecting the derivative of the potential  $V_{,\phi}$ , we have

$$\ddot{\phi} + 3H\dot{\phi} \approx 0, \quad (3.3)$$

whose solution is given by

$$\dot{\phi}(t) = \pm \sqrt{2\rho_{\text{cr}}} \left[ \frac{a_B}{a(t)} \right]^3, \quad (3.4)$$

where  $a_B$  is the scalar factor at the bounce. Substituting the solution (3.4) in Eq. (2.2), we obtain

$$a(t) = a_B \left[ 1 + \frac{24\pi\rho_{\text{cr}}}{m_{\text{Pl}}^4} \frac{(t - t_B)^2}{t_{\text{Pl}}^2} \right]^{1/6}, \quad (3.5)$$

where  $a_B \equiv a(t_B)$  and  $t_B$  is the bounce instant. Equation (3.5) gives the expression for the scale factor in the quantum regime of the Universe. In the above equation,  $t_{\text{Pl}} = 1/m_{\text{Pl}}$  is the Planck time.

With the analytical solution for  $a(t)$ , from (3.4) one finds

$$\dot{\phi}(t) = \pm \frac{\sqrt{2\rho_{\text{cr}}}}{\left[ 1 + \frac{24\pi\rho_{\text{cr}}}{m_{\text{Pl}}^4} (t - t_B)^2/t_{\text{Pl}}^2 \right]^{1/2}}, \quad (3.6)$$

and

$$\phi(t) = \phi_B \pm \frac{m_{\text{Pl}}}{2\sqrt{3}\pi} \operatorname{arcsinh} \left[ \sqrt{\frac{24\pi\rho_{\text{cr}}}{m_{\text{Pl}}^4} \frac{(t - t_B)^2}{t_{\text{Pl}}^2}} \right]. \quad (3.7)$$

It is important to notice that even though the result for the inflaton amplitude Eq. (3.7) is derived close to the bounce and where the inflaton potential is negligible, its validity still extends quite well for a long time interval both before and after the bounce. This is illustrated in Fig. 1, where we show the numerical evolution for the inflaton amplitude  $\phi(t)$  and compare it to the analytical result given by Eq. (3.7). For illustrative purposes, we have considered the quadratic power-law potential, Eq. (2.6) with  $n = 1$ , but the results remain qualitatively similar when considering other potentials. The initial conditions were considered deep in the contracting phase and such that around 147  $e$ -folds of inflation would be produced. This value of  $e$ -folds of inflation was chosen since it is within what is expected for this potential from previous statistical analysis for this form of potential (see, e.g., Refs. [30, 34] for details). The transition time in the contracting and expanding phases,  $t_{\text{tr}}^-$  and  $t_{\text{tr}}^+$ , respectively, defined by  $\dot{\phi}^2(t_{\text{tr}}^\pm)/2 = V(\phi(t_{\text{tr}}^\pm))$ , are marked by the red and green vertical strips, respectively. The bounce is marked by the blue vertical strip. Note that the analytical result for  $\phi(t)$  agrees well with the numerical solution obtained when evolving Eq. (2.5) with the Hubble parameter in LQC given by Eq. (2.2) in the whole region  $t_{\text{tr}}^- \lesssim t \lesssim t_{\text{tr}}^+$ .

### B. Setting the initial conditions

Let us now describe the process of determining the appropriate initial conditions for the evolution of the system and which will determine the inflaton amplitude at the bounce instant,  $\phi_B$ . Having  $\phi_B$  is important because we can straightforwardly relate all relevant post-bounce quantities for our analysis with it, as we are going to show below.

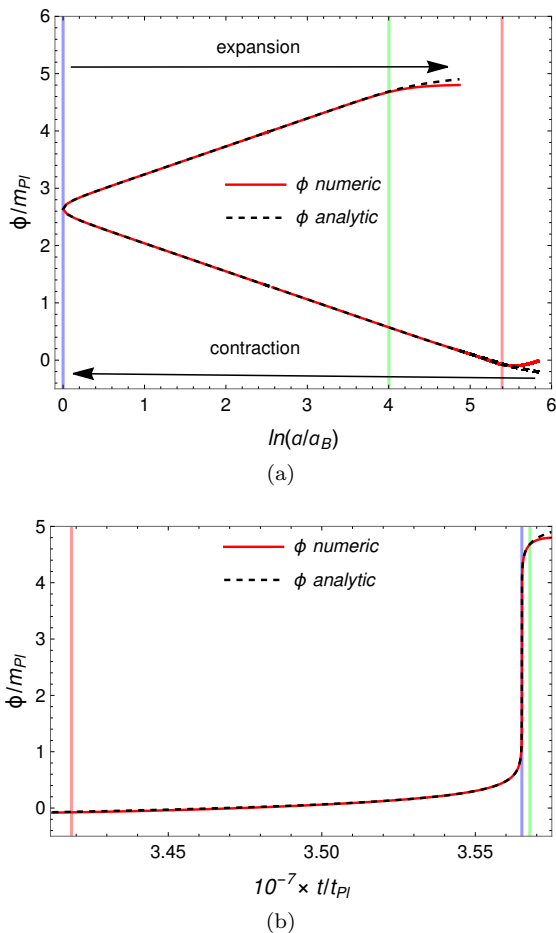


FIG. 1. Comparison of the numerical and analytical results for the inflaton amplitude  $\phi$ . A quadratic power-law potential was considered and initial conditions (set in the contracting phase) such that around 147 e-folds of inflation is generated (see text). The vertical red and green strips indicate the start and end of kinetic energy dominated regime,  $\dot{\phi}^2/2 > V(\phi)$ . The vertical blue strip indicates the bounce instant  $t_B$ . Evolution is shown in terms of both the number of e-folds (panel a) and in terms of the physical time (panel b).

We can start by considering the dynamics at some point in the contracting phase, after the transition time  $t_{tr}^-$ , but still well before the bounce, such that the quantum effects are still negligible. By defining the ratio of the potential energy to kinetic energy,  $\alpha(t) \equiv V/(\dot{\phi}^2/2)$ , we can then look at some instant in the contracting phase given by  $t_{tr}^- < t_\alpha \ll t_B$ , and where the Hubble parameter can be approximated by

$$H(t) \simeq \frac{1 + \alpha(t)}{3(t - t_B)}. \quad (3.8)$$

Taking the time derivative of Eq. (3.8) and equating it to  $-4\pi\dot{\phi}^2/m_{\text{Pl}}^2$ , which is valid in the regime we are considering, we find a direct relation between the potential

and its field derivative,  $V'$ , as given by

$$\frac{V(\phi_\alpha)}{V'(\phi_\alpha)} = \frac{\sqrt{1 + \alpha}}{4\sqrt{3}\pi} m_{\text{Pl}}. \quad (3.9)$$

To obtain Eq. (3.9), we have used the inflaton's equation of motion Eq. (2.5) along also with Eq. (3.8) to eliminate the explicit time dependence in favor of the Hubble parameter and finally that<sup>1</sup>

$$H = -\sqrt{\frac{8\pi}{m_{\text{Pl}}^2} \frac{(1 + \alpha)}{\alpha}} V, \quad (3.10)$$

which follows when using that  $\dot{\phi}^2/2 \equiv V/\alpha$ . Our approximation to estimate  $\phi_B$  now consists of considering that we can take an “average” value for  $\alpha$  and approximate it as a constant  $\bar{\alpha}$ . In this case, for a given value of  $\bar{\alpha}$  within the range  $(0, 1)$  we can readily estimate the inflaton amplitude  $\phi_\alpha \equiv \phi(t_\alpha)$ , for any given potential, when using Eq. (3.9), and also the instant of time  $t_\alpha$  when using Eqs. (3.8) and (3.10) for  $\alpha \rightarrow \bar{\alpha}$ ,

$$t_\alpha - t_B = -\frac{1 + \bar{\alpha}}{3} \sqrt{\frac{3m_{\text{Pl}}^2 \bar{\alpha}}{8\pi(1 + \bar{\alpha})V(\phi_\alpha)}}. \quad (3.11)$$

Here we fix the value for  $\bar{\alpha}$  such that the dynamics will match the one obtained for each potential and which results are available for the potentials we are analyzing. We note that this strategy is analogous to the one adopted, e.g., by the authors of Ref. [33], where the constant value for  $\alpha$  was fixed by matching their numerical results for  $\phi$ , but in the post-bounce regime instead. Here we avoid to apply this to the post-bounce regime and choose to consider the contracting phase instead. This is justified because, as seen from Fig. 1(b), the post-bounce dynamics lasting from the bounce up to the transition time  $t_{tr}^+$  is much shorter than the one lasting from  $t_{tr}^-$  in the contracting phase until the bounce time  $t_B$ . The ratio of energies  $\alpha$  changes much faster in the expanding phase than in the contracting one. Trying to fix  $\alpha$  to match the numerical results in the expanding phase thus implies in requiring a much higher accuracy than the one we can achieve doing the same procedure in the contracting phase.

### C. The post-bounce transition time and the inflaton amplitude

Having both  $\phi_\alpha$  and the instant  $t_\alpha$  for a given value of  $\bar{\alpha}$  by following the above procedure in the contracting phase, we then can use Eq. (3.7) to obtain the inflaton

<sup>1</sup> Note the choice of minus sign for the Hubble parameter is because we are considering the dynamics in the contracting phase, hence,  $H < 0$ .

amplitude at the bounce time,  $\phi_B$ . Given the value for  $\phi_B$ , we can estimate the number of e-folds of inflation. Firstly, the inflaton value at the transition time  $t_{tr}^+$  in the post-bounce regime is determined by using Eq. (3.7) again,

$$\phi(t_{tr}^+) = \phi_B + \frac{m_{\text{Pl}}}{2\sqrt{3}\pi} \operatorname{arcsinh} \left( \sqrt{\frac{24\pi\rho_{\text{cr}}}{m_{\text{Pl}}^4}} \frac{t_{tr}^+ - t_B}{t_{\text{Pl}}} \right). \quad (3.12)$$

We can now consider that at the transition time we have that<sup>2</sup>

$$\dot{\phi}(t_{tr}^+) = \sqrt{2V(\phi(t_{tr}^+))}. \quad (3.13)$$

By using the time derivative of  $\phi(t)$ , Eq. (3.6) at  $t_{tr}^+$  and substituting Eq. (3.12) in Eq. (3.13), we can then numerically<sup>3</sup> solve Eq. (3.13) for the time interval  $t_{tr}^+ - t_B$ . This result then also allows us to obtain  $\phi(t_{tr}^+)$  when substituting the solution for  $t_{tr}^+ - t_B$  back in Eq. (3.12).

#### D. Beginning of the slow-roll inflationary phase

When the slow-roll phase starts at some time  $t_i > t_{tr}^+$ , the Universe is already far from the quantum regime. The potential energy starts to dominate over the kinetic energy giving rise to the inflationary regime. In the following, we use the index ‘‘i’’ to denote the quantities at the beginning of inflation, which corresponds to the moment when the Universe starts accelerating and the equation of state satisfies  $w \leq -1/3$ . In order to obtain the quantities in this moment, we can use the expansion for  $\phi(t)$  which is valid for  $t \simeq t_i$ ,

$$\phi_i \simeq \phi_{tr} + \dot{\phi}_{tr} t_{tr}^+ \ln \frac{t_i}{t_{tr}^+}, \quad (3.14)$$

<sup>2</sup> Note that we could have this equation for both signs positive or negative for  $\dot{\phi}$ . Throughout this paper, we work with the convention of adopting the positive sign for  $\dot{\phi}$ , thus also considering the positive sign in Eq. (3.7) when writing it for  $t = t_{tr}^+$  in Eq. (3.12). This implies that the field is always moving from the left to the right side of the potential. For the power-law and Higgs potentials this choice does not lead to any ambiguity since the potential is symmetric and for any choice of the sign for  $\dot{\phi}$  the field is always climbing the potential when starting the initial conditions deep inside the contracting phase and always close to the minimum of the potential. The Starobinsky potential is asymmetric, but for the standard form, Eq. (2.8), inflation only happens along the flat region, which resides in the right hand side of the potential.

<sup>3</sup> In fact exact analytical expressions for both  $t_{tr}^+ - t_B$  and  $\phi(t_{tr}^+)$  can be obtained from these equations by approximating them by considering that  $t_{tr}^+ - t_B \gg t_{\text{Pl}}$  (see, e.g., Ref. [10] for details in the cases of the quadratic power law and Starobinsky potentials). The solution is in general expressed in terms of Lambert functions. Here we simply choose to directly numerically solve Eq. (3.13), which can in principle be done for any potential in general.

where  $\phi_{tr} \equiv \phi(t_{tr}^+)$ ,  $\dot{\phi}_{tr} \equiv \dot{\phi}(t_{tr}^+)$  and, without loss of generality, we are setting from this point on that  $t_B = 0$ . Likewise for  $\dot{\phi}(t_i)$ , we have that

$$\dot{\phi}_i \simeq \frac{t_{tr}^+}{t_i} \dot{\phi}_{tr}. \quad (3.15)$$

Thus,

$$V(\phi_i) \simeq V(\phi_{tr}) + V_{,\phi}(\phi_{tr}) t_{tr}^+ \dot{\phi}_{tr} \ln \frac{t_i}{t_{tr}^+}. \quad (3.16)$$

Since the accelerated regime,  $\ddot{a} > 0$ , starts at  $w = -1/3$  for the equation of state, then

$$\dot{\phi}_i^2 = V(\phi_i). \quad (3.17)$$

Using Eqs. (3.17) and (3.16) and knowing  $t_{tr}^+$  and  $\phi_{tr}$  obtained from the previous step, we can now numerically solve<sup>4</sup> Eq. (3.17) for the initial time  $t_i$ , which will then determine  $\phi_i$  from Eq. (3.14).

#### E. Number of e-folds $N_{\text{pre}}$ and $N_{\text{infl}}$

The number of e-folds of expansion is defined as,

$$N \equiv \ln \left( \frac{a_{\text{end}}}{a_{\text{init}}} \right), \quad (3.18)$$

where  $a_{\text{init}}$  and  $a_{\text{end}}$  denotes, respectively, the scale factors at the beginning and at the end, respectively, of the corresponding period.

Let us firstly present the results for the pre-inflationary phase, i.e., the expansion lasting from the bounce time to the start of the inflationary phase. The number of e-folds for the pre-inflationary phase is denoted by  $N_{\text{pre}}$ , with  $N_{\text{pre}} \equiv \ln(a_i/a_B)$ , where  $a_B$  and  $a_i$  are the scale factors at the bounce and at the beginning of inflation, respectively. According to what we have done in the previous sections, we can write  $a_i$  as [10]

$$a_i \simeq a_{tr} \left( 1 + t_{tr}^+ H_{tr} \ln \frac{t_i}{t_{tr}^+} \right), \quad (3.19)$$

where  $H_{tr}$  in Eq. (3.19) is obtained from the Friedmann equation considering  $\rho_{tr} = \dot{\phi}_{tr}^2/2 + V(\phi_{tr})$ . Therefore, the number of e-folds of expansion in the pre-inflationary phase can be written as

$$\begin{aligned} N_{\text{pre}} &= \ln \left( \frac{a_i}{a_B} \right) = \ln \left( \frac{a_{tr}}{a_B} \right) + \ln \left( \frac{a_i}{a_{tr}} \right) \\ &\simeq \frac{1}{6} \ln \left( 1 + \frac{24\pi\rho_{\text{cr}}}{m_{\text{Pl}}^4} \frac{(t_{tr}^+)^2}{t_{\text{Pl}}^2} \right) + \ln \left( 1 + t_{tr}^+ H_{tr} \ln \frac{t_i}{t_{tr}^+} \right), \end{aligned} \quad (3.20)$$

<sup>4</sup> Again, it can be found general analytical solutions for Eq. (3.17) which are expressed also in terms of Lambert functions [10], but for practical purposes we just opt to numerically solve Eq. (3.17).

where we have used Eq. (3.5) at  $t = t_{tr}^+$  and Eq. (3.19).

The number of the  $e$ -folds of expansion during the inflationary phase,  $N_{\text{infl}}$ , is defined as,

$$N_{\text{infl}}(\phi) \equiv \ln \left( \frac{a_{\text{end}}}{a_i} \right) \approx \frac{8\pi}{m_{\text{Pl}}^2} \int_{\phi_{\text{end}}}^{\phi_i} \left( \frac{V}{V'} \right) d\phi, \quad (3.21)$$

where in the last term in the above equation we have used the slow-roll approximations, valid during inflation,  $\dot{\phi} \simeq -V_{,\phi}/(3H)$  and  $H^2 \simeq 8\pi V/(3m_{\text{Pl}}^2)$ . The total number of  $e$ -folds lasting from the bounce until the end of inflation is then  $N_{\text{total}} = N_{\text{pre}} + N_{\text{infl}}$ . In Eq. (3.21),  $\phi_i$  is given by Eq. (3.14) and  $\phi_{\text{end}}$ , the scalar field at the end of the inflationary phase, is obtained by the slow-roll coefficient  $\epsilon = -\dot{H}/H^2$  when it is set to one (indicating the end of the accelerated regime). Thus, from  $\epsilon = -\dot{H}/H^2 \simeq (V_{,\phi} m_{\text{Pl}}/V)^2/(16\pi) = 1$ ,  $\phi_{\text{end}}$  can be readily obtained for each of the potential forms we are considering. The results are explicitly given below.

### 1. The Power-law monomial potentials

From Eq. (3.21),  $N_{\text{infl}}$  in the case of monomial potentials is given by

$$N_{\text{infl}} = \frac{2\pi}{n m_{\text{Pl}}^2} (\phi_i^2 - \phi_{\text{end}}^2), \quad (3.22)$$

with  $\phi_{\text{end}}$  given by

$$\phi_{\text{end}}^2 = \frac{n^2}{4\pi} m_{\text{Pl}}^2. \quad (3.23)$$

### 2. The Higgs-like symmetry breaking potential

For the Higgs-like potential we have that

$$N_{\text{infl}} = \frac{2\pi}{m_{\text{Pl}}^2} \left[ \frac{\phi_i^2 - \phi_{\text{end}}^2}{2} - v^2 \ln \frac{\phi_i}{\phi_{\text{end}}} \right], \quad (3.24)$$

and

$$\phi_{\text{end}} = \pm \sqrt{v^2 + \frac{m_{\text{Pl}}^2}{2\pi} \pm \frac{m_{\text{Pl}}^2}{2\pi} \sqrt{1 + \frac{4\pi v^2}{m_{\text{Pl}}^2}}}, \quad (3.25)$$

where the signs positive and negative correspond to the large and small-field cases, respectively.

### 3. The Starobinsky potential

For the Starobinsky potential we obtain that

$$N_{\text{infl}} = \frac{3}{4} \left( e^{\sqrt{\frac{16\pi}{3}} \frac{\phi_i}{m_{\text{Pl}}}} - e^{\sqrt{\frac{16\pi}{3}} \frac{\phi_{\text{end}}}{m_{\text{Pl}}}} \right) + \frac{\sqrt{3\pi}}{m_{\text{Pl}}} (\phi_i - \phi_{\text{end}}), \quad (3.26)$$

where

$$\phi_{\text{end}} = m_{\text{Pl}} \sqrt{\frac{3}{16\pi}} \ln \left( 1 + \frac{2}{\sqrt{3}} \right). \quad (3.27)$$

Having derived and collect all relevant equations, we are now in condition to present our results in the following section.

## IV. RESULTS

As explained in Sec. III B, we first need to set an appropriate value for the ratio  $\bar{\alpha}$  of potential to kinetic energy in the contracting phase. We illustrate this by comparing the results generated for the number of  $e$ -folds, Eq. (3.21) within our approach to those obtained through the statistical analysis produced in Ref. [30]. In Ref. [30], which follows the proposal initiated by the authors of Ref. [34], initial conditions are generated deep inside the contracting phase, where  $\rho_\phi \ll \rho_{\text{cr}}$ , and the inflaton is oscillating around the minimum of its potential. The number of  $e$ -folds of inflation is then obtained by taking a large number of random initial conditions satisfying these conditions and each one of them is evolved up to the end of inflation. The probability distribution function (PDF) for each potential is obtained, from which statistical predictions for the number of  $e$ -folds are derived. In Ref. [30] results were obtained for the power-law potential with  $n = 1, 2, 3$  and also for the Higgs-like potential for different values for the VEV  $v$ . These results of Ref. [30] are indicated, for comparison, by the data points with the error bars shown in Fig. 2, for the case of the power-law potential, and in Fig. 3, for the case of the Higgs-like potential.

From the results shown in Fig. 2, we see that the results very reasonably fit the ‘‘data’’ points, with a difference of less than 5%, for the choice<sup>5</sup>  $\bar{\alpha} = 1/3$ . The same choice of  $\bar{\alpha}$  is also seen to reproduce well the results for the Higgs-like potential, for many different values for  $v$ , as shown in Fig. 3. Note that for the Higgs-like potential curves do not quite agree with the ‘‘data’’ points for the pre-inflationary number of  $e$ -folds, but the qualitative agreement is still very good, again within less than 5% differences<sup>6</sup>.

<sup>5</sup> We note that the same value for the constant  $\alpha$  given by 1/3 was, coincidentally, also found by the authors of Ref. [33], though matching their numerical results that were obtained in the post-bounce phase.

<sup>6</sup> We notice that for all data points shown in the figures, the error bars are the one-standard deviation from the average values.



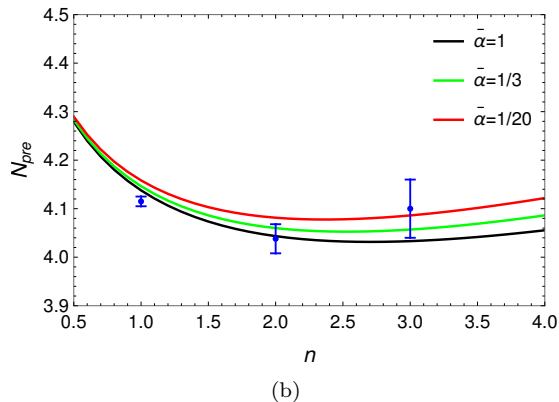
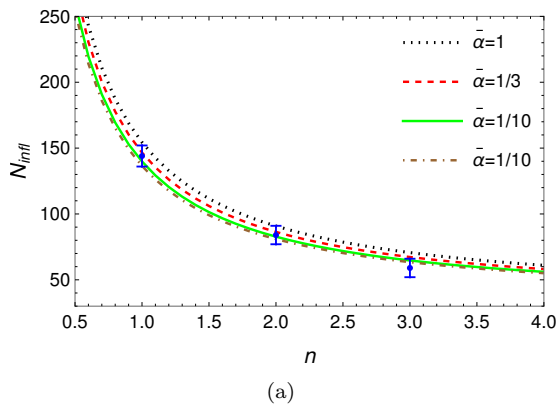


FIG. 2. The numerical results for the number of e-folds of inflation (panel a) and for the number of e-folds for the pre-inflationary regime lasting from the bounce until the beginning of inflation (panel b) obtained through the method described in Sec. III E when applied to the monomial power-law potential Eq. (2.6). The “data” points show the results obtained in Ref. [30].

Given the results shown in Figs. 2 and 3, all our subsequent analysis will be done by choosing  $\bar{\alpha} = 1/3$ . Recalling that  $\alpha$  is related to the equation of state by the relation

$$\begin{aligned} w &= \frac{\dot{\phi}^2/2 - V(\phi)}{\dot{\phi}^2/2 + V(\phi)} \\ &= \frac{1 - \alpha}{1 + \alpha}, \end{aligned} \quad (4.1)$$

then the choice  $\bar{\alpha} = 1/3$  is also equivalent of considering the moment  $t_\alpha$  in the contracting phase where  $w = 1/2$ .

Figures 2 and 3 already show some revealing features. One recalls that one typically requires at least around 80 e-folds of total expansion from the bounce to the end of inflation in order for the quantum effects on the spectra to be sufficiently diluted [10]. On the contrary, if the total expansion lasts less than this minimum, the LQC effects on the spectra would already be visible. This limitation, which is a consequence of the effects of LQC on the power spectrum, will be detailed below in the next section. From Fig. 2(a), therefore, it indicates that

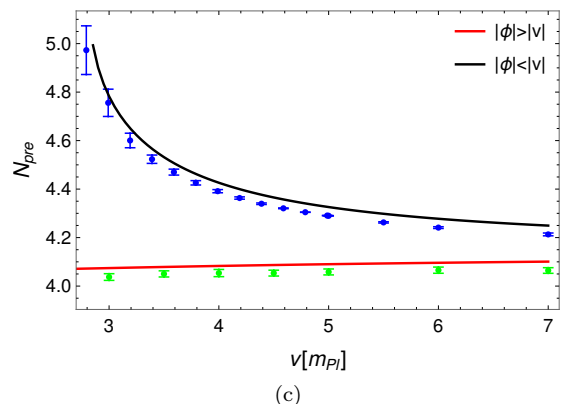
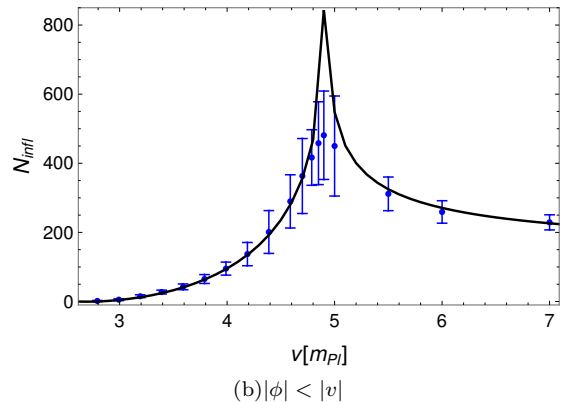
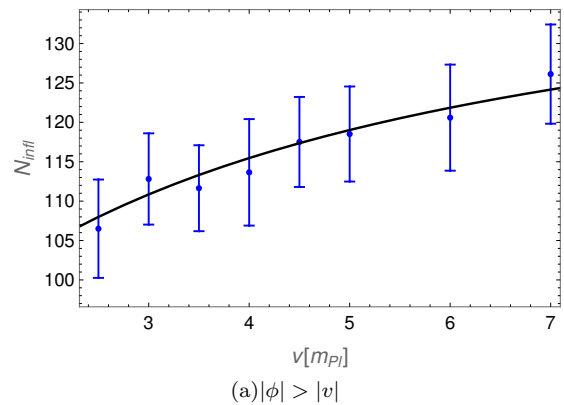


FIG. 3. The numerical results for the number of e-folds of inflation in the case of the Higgs-like potential when inflation happens in the large-field portion of the potential,  $|\phi| > |v|$  (panel a), and for inflation happening around the plateau region,  $|\phi| < |v|$  (panel b). The number of e-folds for the pre-inflationary regime lasting from the bounce until the beginning of inflation is shown in the panel c. The data points are the results obtained using the methods described in Ref. [30]. All curves here were obtained by setting  $\bar{\alpha} = 1/3$  within the procedure described in Sec. III B.

monomial power-law potentials with a fifth power in the inflaton ( $n = 2.5$ ) and higher are not favored due to the small amount of expansion predicted from them. For the quadratic potential ( $n = 1$ ) the situation is quite different. We obtain  $N_{\text{inf}} \sim 147$ , in agreement with previous

results obtained in Ref. [34]. Despite being in agreement with current CMB data, such high value for  $N_{\text{infl}}$  does not lead to good prospects in observing signals from the high energy regime on CMB data. On the other hand, for the quartic model ( $n = 2$ ) we obtain  $N_{\text{infl}} \sim 87$ . This value, while providing satisfactory number of  $e$ -folds of inflation, it also allows for better prospects concerning potentially observable signals from the quantum regime of LQC on future CMB measurements. Fig. 3(a), which shows our results for the Higgs-like potential when inflation happens on the large-field portion of the potential, i.e.,  $|\phi| > |v|$ , the number of  $e$ -folds is always larger than  $N_{\text{infl}} \sim 87$ , whose value is approached when  $v \rightarrow 0$  and the model is analogous to the quartic monomial potential. However, when inflation happens in the plateau region of the potential, i.e., when  $|\phi| < |v|$ , the number of  $e$ -folds tends initially to increase with the value of the VEV  $v$ , up to around  $v \sim 5m_{\text{Pl}}$ , after what it drops and tends to asymptote around  $N_{\text{infl}} \sim 200$ . This behavior was already hinted in the analysis done in Ref. [30] but it becomes clear now in the results shown in Fig. 3(b). This apparently odd behavior has a simple explanation. For small VEV values, the plateau region of the potential is small and it is difficult to localize the inflaton in that small field region of the potential and the number of  $e$ -folds of inflation tends to be small. As the VEV increases, it becomes more likely for inflation to happen closer to the flatter top of the potential and the number of  $e$ -folds of inflation increases<sup>7</sup>. However, for even larger values for the VEV, it becomes again less likely that the dynamics would put the inflaton too close to the top of the potential and the number of  $e$ -folds decreases. Our results indicates that there is an optimum value for the VEV for inflation having a maximum number of  $e$ -folds for a Higgs-like potential in the context of LQC and this value for the VEV is around  $v \sim 5m_{\text{Pl}}$ . On the other hand, our results also show that for  $v \lesssim 3m_{\text{Pl}}$ , there are essentially no more initial conditions leading to inflation starting and ending in the plateau region, which also agrees with the findings of Ref. [58].

Our results, including also the ones for the Starobinsky potential Eq. (2.8), are summarized in Tabs. I to IV. We have chosen the cases of a quadratic, a quartic and a sextic monomials potentials for illustration, along with some representative cases of the Higgs-like potential and then the Starobinsky potential.

In Tabs. I and II we give the results for the various quantities which were defined in the previous section, in particular the numerical prediction for the amplitude for

<sup>7</sup> It should be noticed that the number of  $e$ -folds in Fig. 3(b) appears to grow very sharp at around  $v \simeq 5m_{\text{Pl}}$ , we expect the real situation to display a smoother maximum as actually indicated by the numerical data. This is because there is always Gaussian stochastic quantum fluctuations acting on the background inflaton field [58]. These fluctuations make unlikely for the inflaton to be precisely localized at the top of the maximum of the potential at  $\phi = 0$ .

the inflaton field at the bounce,  $\phi_{\text{B}}$ . This is important, since all other quantities, in particular the point where inflation starts, depends on this value. In a sense, we see that this is equivalent of providing the initial conditions at the bounce time. The subsequent evolution of the Universe is then completely determined from these initial conditions, in special the inflationary regime. In this case, knowing the initial conditions at the bounce, we have shown that it completely determines the duration of inflation for any given potential. The total duration of inflation is a prediction here and no longer a statistical result as considered for example in Refs. [30, 34–37]. The predicted values for the duration of the pre-inflationary phase and inflation are shown in Tabs. III and IV.

From the results shown in Table III and IV, we can see that for all models studied the number of pre-inflationary  $e$ -folds, which consider the expansion from the bounce to the beginning of the slow-roll inflation, is always  $N_{\text{pre}} \sim 4 - 5$ , which agrees with Ref. [30] and other previous references. This is a consequence of the bounce being dominated by the kinetic energy of the inflaton field, thus, being weakly dependent on the form of its potential. For the number of inflationary  $e$ -folds, we also obtain results generically in agreement with those obtained in Ref. [30]. In particular, we can observe that for the Starobinsky potential  $N_{\text{infl}} \sim 10^9$ , i.e., the duration of slow-roll inflation is longer compared to the other models. This is consistent with the results shown, e.g., in Ref. [37], which follows the determination for the number of  $e$ -folds of inflation originally proposed in Ref. [34] and which was also considered in Ref. [30]. This happens for positive values of the scalar field at the beginning of inflation, i.e., where the potential have a plateau [59]. As discussed in Ref. [37], LQC dynamics automatically provides highly energetic field configurations at the onset of inflation. Consequently, in these cases the inflaton field is “pushed” away on the plateau, leading to a very long phase of slow-roll inflation. For the monomials power-law potentials, as already seen in a previous work [30], increasing the power  $n$  implies in a decreasing of the number of  $e$ -folds.

## V. CONSTRAINING THE BARBERO-IMMIRZI PARAMETER

As previously discussed, the Barbero-Immirzi parameter is strictly a free parameter of the theory. Therefore, it is important to find ways to constraint its value. In this section we study how the prediction for the number of  $e$ -folds in LQC helps in setting possible constraints on the Barbero-Immirzi parameter  $\gamma$ .

### A. The power spectrum in LQC

The quantum bounce changes the scalar power spectrum by a correction term which depends on the char-

TABLE I. Numerical values obtained for the three forms of monomials potentials and the Starobinsky potential.

Model	$V_0/m_{\text{Pl}}^4$	$\phi_{\text{B}}/m_{\text{Pl}}$	$t_{\text{tr}}^+/t_{\text{Pl}}$	$\phi_{\text{tr}}/m_{\text{Pl}}$	$(10^6)\dot{\phi}_{\text{tr}}/m_{\text{Pl}}^2$	$t_i/t_{\text{Pl}}$	$\phi_i/m_{\text{Pl}}$
Quadratic	$1.355 \times 10^{-12}$	2.72	$2.9 \times 10^4$	4.72	5.6	$4.1 \times 10^4$	4.84
Quartic	$1.373 \times 10^{-13}$	3.19	$2.3 \times 10^4$	5.22	7.1	$3.2 \times 10^4$	5.27
Sextic	$4.563 \times 10^{-15}$	3.65	$2.3 \times 10^4$	5.68	7.1	$3.1 \times 10^4$	5.73
Starobinsky	$1.497 \times 10^{-13}$	2.65	$3.0 \times 10^5$	5.10	0.5	$4.2 \times 10^5$	5.16

TABLE II. Numerical values obtained for the Higgs-like potential, considering some illustrative values for the VEV.

Model	$V_0/m_{\text{Pl}}^4$	$\phi_{\text{B}}/m_{\text{Pl}}$	$t_{\text{tr}}^+/t_{\text{Pl}}$	$\phi_{\text{tr}}/m_{\text{Pl}}$	$(10^6)\dot{\phi}_{\text{tr}}/m_{\text{Pl}}^2$	$t_i/t_{\text{Pl}}$	$\phi_i/m_{\text{Pl}}$
Higgs-like ( $ \phi_{\text{B}}  >  v = 3.5m_{\text{Pl}} $ )	$2.867 \times 10^{-14}$	6.27	$2.4 \times 10^4$	8.30	6.8	$3.3 \times 10^4$	8.35
Higgs-like ( $ \phi_{\text{B}}  >  v = 4.0m_{\text{Pl}} $ )	$2.384 \times 10^{-14}$	6.76	$2.4 \times 10^4$	8.80	6.7	$3.4 \times 10^4$	8.85
Higgs-like ( $ \phi_{\text{B}}  >  v = 4.5m_{\text{Pl}} $ )	$2.010 \times 10^{-14}$	7.25	$2.5 \times 10^4$	9.29	6.6	$3.4 \times 10^4$	9.35
Higgs-like ( $ \phi_{\text{B}}  <  v = 3.5m_{\text{Pl}} $ )	$6.424 \times 10^{-14}$	-0.79	$9.0 \times 10^4$	1.46	1.8	$1.3 \times 10^5$	1.52
Higgs-like ( $ \phi_{\text{B}}  <  v = 4.0m_{\text{Pl}} $ )	$5.245 \times 10^{-14}$	-1.30	$6.6 \times 10^4$	0.90	2.5	$9.4 \times 10^4$	0.96
Higgs-like ( $ \phi_{\text{B}}  <  v = 4.5m_{\text{Pl}} $ )	$4.254 \times 10^{-14}$	-1.80	$5.6 \times 10^4$	0.37	2.9	$7.9 \times 10^4$	0.43

TABLE III. Number of  $e$ -folds obtained through the analytical analysis for the same models considered in Tab. I.

Model	$N_{\text{pre}}$	$N_{\text{infl}}$
Quadratic	4.15	146.55
Quartic	4.06	86.36
Sextic	4.06	67.30
Starobinsky	4.92	$1.10 \times 10^9$

TABLE IV. Number of  $e$ -folds obtained for the Higgs-like potential, assuming different values for the VEV.

Model	$N_{\text{pre}}$	$N_{\text{infl}}$
Higgs-like ( $ \phi_{\text{B}}  >  v = 3.5m_{\text{Pl}} $ )	4.08	113.31
Higgs-like ( $ \phi_{\text{B}}  >  v = 4.0m_{\text{Pl}} $ )	4.08	115.46
Higgs-like ( $ \phi_{\text{B}}  >  v = 4.5m_{\text{Pl}} $ )	4.09	117.35
Higgs-like ( $ \phi_{\text{B}}  <  v = 3.5m_{\text{Pl}} $ )	4.53	32.64
Higgs-like ( $ \phi_{\text{B}}  <  v = 4.0m_{\text{Pl}} $ )	4.43	95.66
Higgs-like ( $ \phi_{\text{B}}  <  v = 4.5m_{\text{Pl}} $ )	4.37	235.92

acteristic scale at the bounce. This characteristic scale is the shortest scale (or largest wavenumber, namely  $k_{\text{B}}$ ) that feels the spacetime curvature during the bounce. In previous works (see for instance, Ref. [51]), precise constraints on the correction term in the scalar power spectrum of LQC was obtained using the recent CMB data,

providing limits on the characteristic scale  $k_{\text{B}}$ . It happens that this scale is a function of the Barbero-Immirzi parameter and the number of  $e$ -folds of expansion from the bounce until today,  $N_{\text{T}}$ . Therefore, in the following we use such observational constraints on  $k_{\text{B}}$  in order to impose limits on the value of  $\gamma$  as a function of the  $e$ -fold number.

In addition to the modifications at the background level from LQC, at the perturbative level modifications are also expected, especially from relevant modes which have physical wavelengths comparable to the curvature radius at the bounce time. Unlike what happens in GR, where it is usually assumed that the pre-inflationary dynamics does not have any effect on modes observable in the CMB, in LQC the situation is different. Modes that experience curvature are excited in the Planck regime around the bounce time. The main effect at the onset of inflation is that the quantum state of perturbations is populated by excitations of these modes over the Bunch-Davis vacuum. As a consequence, the scalar curvature power spectrum in LQC gets modified with respect to GR, such that it can be written as (see Ref. [10] for more details)

$$\Delta_{\mathcal{R}}(k) = |\alpha_k + \beta_k|^2 \Delta_{\mathcal{R}}^{GR}(k). \quad (5.1)$$

$$= (1 + 2|\beta_k|^2 + 2\text{Re}(\alpha_k \beta_k^*)) \Delta_{\mathcal{R}}^{GR}(k). \quad (5.2)$$

In Eq. (5.1)  $\alpha_k$  and  $\beta_k$  are the Bogoliubov coefficients, where the pre-inflationary effects are codified, and  $\Delta_{\mathcal{R}}^{GR}$  is the GR form for the power spectrum. In GR with the Bunch-Davis vacuum, the Bogoliubov coefficients in Eq. (5.1) should reduce simply to  $\alpha_k \rightarrow \alpha_k^{\text{BD}} = 1$ , and  $\beta_k \rightarrow \beta_k^{\text{BD}} = 0$ . In LQC, the change of the spectrum can

be seen exactly as a result of the change of the vacuum state with respect to the GR case, since  $|\beta_k|^2 \equiv n_k$  is associated with the number of excitations in the mode  $k$ .

The Eq. (5.1) can also be parametrized as

$$\Delta_{\mathcal{R}}(k) = (1 + \delta_{PL})\Delta_{\mathcal{R}}^{GR}(k), \quad (5.3)$$

where the factor  $\delta_{PL}$  is a scale ( $k$ -)dependent correction given by

$$\begin{aligned} \delta_{PL} = & \left[ 1 + \cos\left(\frac{\pi}{\sqrt{3}}\right) \right] \operatorname{csch}^2\left(\frac{\pi k}{\sqrt{6}k_B}\right) \\ & + \sqrt{2} \sqrt{\cosh\left(\frac{2\pi k}{\sqrt{6}k_B}\right) + \cos\left(\frac{\pi}{\sqrt{3}}\right)} \cos\left(\frac{\pi}{2\sqrt{3}}\right) \\ & \times \operatorname{csch}^2\left(\frac{\pi k}{\sqrt{6}k_B}\right) \cos(2k\eta_B + \varphi_k), \end{aligned} \quad (5.4)$$

where

$$\varphi_k \equiv \arctan \left\{ \frac{\operatorname{Im}[\Gamma(a_1)\Gamma(a_2)\Gamma^2(a_3 - a_1 - a_2)]}{\operatorname{Re}[\Gamma(a_1)\Gamma(a_2)\Gamma^2(a_3 - a_1 - a_2)]} \right\}, \quad (5.5)$$

with  $a_1, a_2, a_3$  defined as  $a_{1,2} = (1 \pm 1/\sqrt{3})/2 - ik/(\sqrt{6}k_B)$  and  $a_3 = 1 - ik/(\sqrt{6}k_B)$ . In particular,  $\eta_B$  is the conformal time at the bounce and  $k_B = \sqrt{\rho_c a_B} \sqrt{8\pi}/m_{\text{Pl}}$  is the characteristic scale also at the bounce.

From the above equations, we identify

$$\begin{aligned} 2|\beta_k|^2 = & \left[ 1 + \cos\left(\frac{\pi}{\sqrt{3}}\right) \right] \operatorname{csch}^2\left(\frac{\pi k}{\sqrt{6}k_B}\right), \quad (5.6) \\ 2\operatorname{Re}(\alpha_k \beta_k^*) = & \sqrt{2} \sqrt{\cosh\left(\frac{2\pi k}{\sqrt{6}k_B}\right) + \cos\left(\frac{\pi}{\sqrt{3}}\right)} \\ & \times \cos\left(\frac{\pi}{2\sqrt{3}}\right) \operatorname{csch}^2\left(\frac{\pi k}{\sqrt{6}k_B}\right) \cos(2k\eta_B + \varphi_k). \end{aligned} \quad (5.7)$$

The term  $\cos(2k\eta_B + \varphi_k)$  in Eq. (5.7) oscillates very fast, having negligible effect when averaging out in time. Therefore, for practical purposes, in observable quantities the factor  $\delta_{PL}$  can be simply considered as being given by

$$\delta_{PL} = \left[ 1 + \cos\left(\frac{\pi}{\sqrt{3}}\right) \right] \operatorname{csch}^2\left(\frac{\pi k}{\sqrt{6}k_B}\right). \quad (5.8)$$

Note that in this case  $\delta_{PL}$  can simply be identified with  $2n_k$ , i.e., with the number of excitations in the mode  $k$  which appears as a consequence of the quantum bounce in LQC. It is due to this correction term that in LQC, in order to be consistent with observations, the Universe must have expanded extra 21  $e$ -folds allowing these scale-dependent features to get sufficiently diluted, as discussed in details in Refs. [10, 51].

## B. The Barbero-Immirzi parameter as a function of the number of $e$ -folds

The total number of  $e$ -folds of expansion from the moment of the bounce until today,  $N_{\text{T}}$ , is related to the LQC parameter  $k_B$ . By assuming an upper bound on  $k_B$ , it can be translated into constraints on the total number of  $e$ -folds. We are interested in finding an upper bound value for  $k_B$ , which implies in a lower value for the number of  $e$ -folds. In Ref. [51], for example, constraints on the parameter  $k_B$  were obtained from CMB data. Since  $k_B$  is related to  $\gamma$ , these results can be translated into constraints in the parameter  $\gamma$ .

The relation between  $k_B$  and the number of  $e$ -folds is given by the equation,

$$k_B \equiv \frac{\sqrt{8\pi\rho_{\text{cr}}a_B}}{m_{\text{Pl}}} = m_{\text{Pl}} \left( \frac{\sqrt{3}}{4\pi\gamma^3} \right)^{1/2} e^{-N_{\text{T}}}, \quad (5.9)$$

where we have used Eq. (2.3) and in the above equation  $N_{\text{T}} = \ln(a_0/a_B)$  is the total number of  $e$ -folds from the bounce until today. Note that in Eq. (5.9) we have used the standard convention of setting the scale factor today as one,  $a_0 = 1$ .

It happens that the CMB observations constraint directly the value of  $k_B$  by imposing a limit in the correction term given by Eq. 5.8. An updated observation constraint on  $k_B$  was obtained in Ref. [51], which leads to  $k_B < 1.9 \times 10^{-4} \text{Mpc}^{-1}$  at  $1\sigma$ . Note that this constraint is independent of the value of the Barbero-Immirzi parameter and should be valid for any value for  $\gamma$ . Using Eq. (5.9), it translates into a lower limit on  $N_{\text{T}}$  depending on the value for the Barbero-Immirzi parameter, that is described by

$$N_{\text{T}} \gtrsim 139 - \frac{3}{2} \ln(\gamma). \quad (5.10)$$

Note that  $N_{\text{T}}$  can be expressed as

$$\begin{aligned} N_{\text{T}} = \ln\left(\frac{a_0}{a_B}\right) &= \ln\left(\frac{a_i}{a_b} \frac{a_{\text{end}}}{a_i} \frac{a_{\text{reh}}}{a_{\text{end}}} \frac{a_0}{a_{\text{reh}}}\right), \\ &= N_{\text{pre}} + N_{\text{infl}} + N_{\text{reh}} + \ln\left(\frac{a_0}{a_{\text{reh}}}\right), \end{aligned} \quad (5.11)$$

where  $a_i$ ,  $a_{\text{end}}$  and  $a_{\text{reh}}$  are the scale factors at the beginning of inflation, at the end of inflation and at the end of the reheating phase, respectively, while  $N_{\text{reh}}$  is the duration of the reheating phase. We also have that [60]

$$\frac{a_0}{a_{\text{reh}}} = \left( \frac{11g_{s,\text{reh}}}{43} \right)^{\frac{1}{3}} \frac{T_{\text{reh}}}{T_{\text{CMB},0}}, \quad (5.12)$$

where  $T_{\text{reh}}$  is the reheating temperature,  $T_{\text{CMB},0}$  is the temperature of the CMB today and  $g_{s,\text{reh}}$  is the effective number of relativistic degrees of freedom for entropy at the end of reheating. Considering the case of instantaneous reheating at the end of inflation (i.e., neglecting the typically unknown physics at reheating),  $N_{\text{reh}} \approx 0$  and

we can associate  $T_{\text{reh}}$  with the inflaton potential energy density at the end of inflation,  $V_{\text{end}}$ , as

$$T_{\text{reh}} \simeq \left( \frac{30}{g_{\text{reh}} \pi^2} \right)^{\frac{1}{4}} (1 + \kappa)^{\frac{1}{4}} V_{\text{end}}^{\frac{1}{4}}, \quad (5.13)$$

where  $g_{\text{reh}}$  is the effective number of relativistic degrees of freedom for energy at full thermalization. In Eq. (5.13),  $\kappa$  is the ratio of kinetic energy to potential energy during inflation. At the end of inflation,  $\kappa = 1/2$ . By taking both  $g_{s,\text{reh}}$  and  $g_{\text{reh}}$  to be close of those for the standard model of particle physics,  $g_{s,\text{reh}} \simeq g_{\text{reh}} \sim 100$ , we obtain that  $\ln(a_0/a_{\text{reh}}) \sim 60$ . Thus, Eq. (5.10) can also be written as a lower bound for  $N_{\text{pre}} + N_{\text{infl}}$ ,

$$N_{\text{pre}} + N_{\text{infl}} \gtrsim 79 - \frac{3}{2} \ln(\gamma). \quad (5.14)$$

Adding the reheating details after inflation only makes the above relation more restrictive. Thus, we can use Eq. (5.14) as an overall lower bound for the total number of  $e$ -folds from the bounce until the end of inflation as a function of the Barbero-Immirzi parameter. By considering the value for  $\gamma$  as given by the value suggested by the black hole entropy [52],  $\gamma \simeq 0.2375$ , we then obtain that  $N_T \gtrsim 141$  and  $N_{\text{pre}} + N_{\text{infl}} \gtrsim 81$ . Recalling also that the number of  $e$ -folds relevant from the CMB observations (e.g., at a pivot scale  $k_* = 0.05/\text{Mpc}$ ) is given by [61]

$$N_* \simeq 61 + \frac{2}{3} \ln \left( \frac{V_*^{1/4}}{10^{16} \text{GeV}} \right) + \frac{1}{3} \ln \left( \frac{T_{\text{reh}}}{10^{16} \text{GeV}} \right), \quad (5.15)$$

which typically leads to  $N_* \sim 50 - 60$  for the necessary number of  $e$ -folds of inflation. As we have seen that  $N_{\text{pre}} \sim 4$ , which is very weakly dependent on the form of the inflaton potential, then  $N_*$  can comfortably fit in the estimated lower bound  $N_{\text{pre}} + N_{\text{infl}} \gtrsim 81$ .

In the following we analyze the general behaviour of the number of  $e$ -folds  $N_{\text{pre+infl}} = N_{\text{pre}} + N_{\text{infl}}$  lasting from the bounce until the end of inflation, as a function of  $\gamma$ . The general expressions for  $N_{\text{pre}}$  and  $N_{\text{infl}}$  were derived in the previous section. Next, we will consider how  $N_{\text{pre+infl}}$  changes by varying the Barbero-Immirzi parameter and also by considering the overall lower bound given by Eq. (5.14).

### C. Results for the Barbero-Immirzi parameter

The behavior of the number of  $e$ -folds from the bounce to the end of inflation as a function of  $\gamma$  for each potential considered in this paper is shown in Figs. 4 and 5. We show in Fig. 4(a) the case of monomial power-law potentials. We consider a sufficiently long range of representative values for  $\gamma$  (the range  $0 \lesssim \gamma \lesssim 10$  typically corresponds to the interval most considered in the literature [41–45]). The almost horizontal gray lines in Figs. 4 and 5 show the lower limit on  $N_{\text{pre+infl}}(\gamma)$  set by

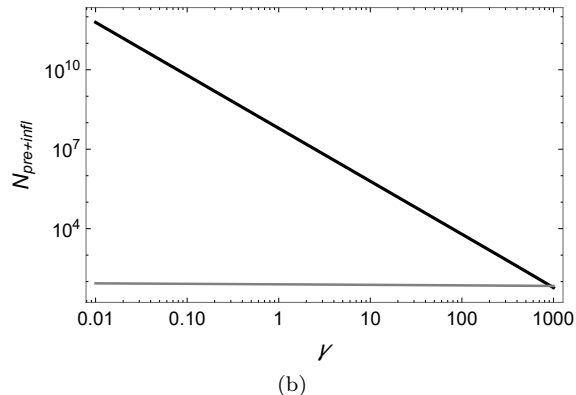
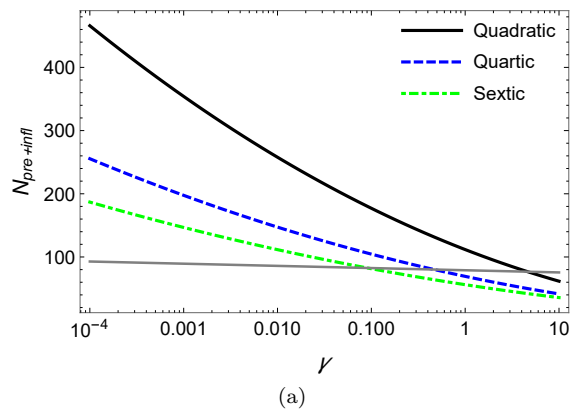


FIG. 4. Number of pre-inflationary plus inflationary  $e$ -folds,  $N_{\text{pre+infl}}$ , for the potentials considered, varying the Barbero-Immirzi parameter. The almost horizontal gray lines show the lower limit on  $N_{\text{pre+infl}}(\gamma)$  set by Eq. (5.14). Panel (a): Power-law potentials; Panel(b): Starobinsky potential.

Eq. (5.14). In all cases it is observed that the smaller the value of  $\gamma$ , the greater the value of  $N_{\text{pre+infl}}$ . The quadratic case ( $n = 1$ ) has a value for  $N_{\text{pre+infl}}$  which is too large for almost the entire interval of  $\gamma$ . However, the quartic ( $n = 2$ ) and sextic ( $n = 3$ ) cases approach the limit of 81  $e$ -folds for smaller values of  $\gamma$ . For the quartic case ( $n = 2$ ), we get that for  $\gamma \sim 0.46$ ,  $N_{\text{pre+infl}}$  reaches the value of 81  $e$ -folds. For the sextic case ( $n = 3$ ), we get that for  $\gamma \sim 0.1$ , the number of  $e$ -folds reaches the limiting value  $N_{\text{pre+infl}} = 81$  and quickly drops below this value as  $\gamma$  increases. We can see that, although for the usual value of the Barbero-Immirzi parameter the sextic potential in LQC is in strong tension with the observations, for smaller values of the parameter,  $\gamma < 0.1$ , it can be consistent.

Complementing these results, we show in Fig. 4(b) the results for the number of  $e$ -folds as a function of  $\gamma$  for the Starobinsky potential. We can see that, again, this corresponds to the case that presents the highest values for  $N_{\text{pre+infl}}$ <sup>8</sup>. We analyzed what value for the  $\gamma$  parameter

<sup>8</sup> See, for example, Ref. [37] for an analysis on the duration of the

would lead to the limiting value of  $N_{\text{pre+infl}} = 81$ . The numerical results shows that in this case the value of the Barbero-Immirzi parameter would be around  $\gamma \sim 1000$ , as can be seen in Fig. 4(b). Note that it corresponds to a value of  $\gamma$  completely inconsistent to the acceptable scales in LQG.

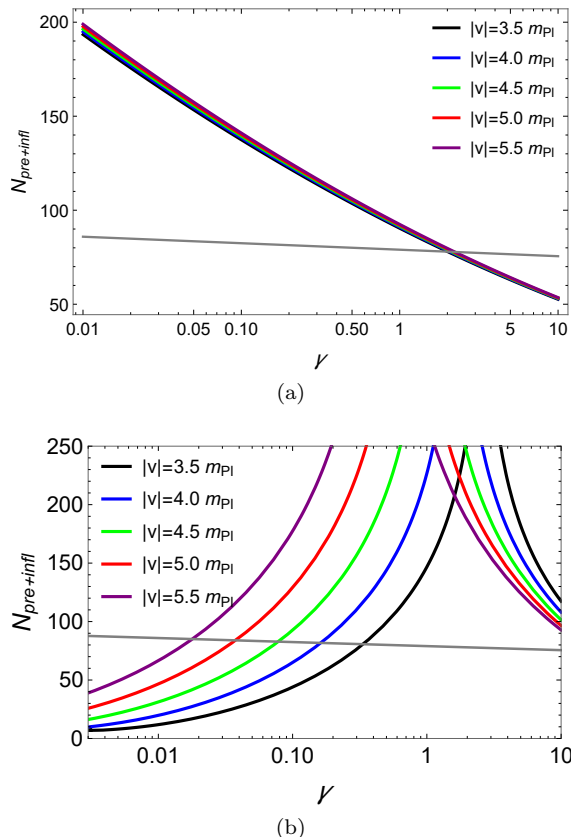


FIG. 5. Number of  $e$ -folds,  $N_{\text{pre+infl}}$ , as a function of the Barbero-Immirzi parameter for the Higgs-like potential with different values of the VEV. The almost horizontal gray lines show the lower limit on  $N_{\text{pre+infl}}(\gamma)$  set by Eq. (5.14). Panel (a): The results for the large field case  $|\phi| > |v|$ ; Panel (b): The results for the small field case  $|\phi| < |v|$ .

To complete our analysis, the results for the Higgs-like potential is shown in Fig. 5. The number of  $e$ -folds as a function of  $\gamma$  for the large field case is shown in Fig. 5(a), while for the small field case it is shown in Fig. 5(b). In both cases, representative values for the VEV are considered. We observe from Fig. 5(a), which is for the large field case, that  $N_{\text{pre+infl}}$  decreases when  $\gamma$  increases. For all VEVs considered, we observe a similar behaviour and we see that the limit  $N_{\text{pre+infl}} = 81$  occurs when  $\gamma \approx 1.15$ . On the other hand, for the small field case, shown in Fig. 5(b), it is possible to observe that the

higher is the VEV, the higher is the number of  $e$ -folds for each value of  $\gamma$ , up to some critical value for  $\gamma$ , above which the number of  $e$ -folds decreases. The decreasing behavior for the number of  $e$ -folds seen here, and that happens above some value of  $\gamma$ , is consequence of the effect already discussed in connection to the one seen in Fig. 3(b). Increasing  $\gamma$  changes the point (VEV) where the number of  $e$ -folds peaks when inflation happens in the plateau region of the potential. For VEVs larger than around  $7m_{\text{Pl}}$ , the number of  $e$ -folds drops below the lower bound set by Eq. (5.14) for  $\gamma \sim 10$ , but for even higher VEVs, the lower bound will be reached for much smaller values of  $\gamma$ .

The results given above show that for different values of  $\gamma$  the predictions for observational signals of LQC in CMB are considerably different. We see that the consistency of the models with the current data depends strongly on the value of this parameter. This motivates and highlights the importance of a careful analysis of the role of the Barbero-Immirzi parameter in these scenarios.

## VI. CONCLUSIONS

It is well known that the primordial power spectrum is a quantity that can relate the theory of the early Universe with the observations. Previous works in the literature have shown that the predictions for the power spectrum in the context of LQC receive a correction term with respect to the predictions in the context of GR. As shown in Ref. [10], due to this correction term, models in the context of LQC requires a minimum amount of  $\sim 81$   $e$ -folds of expansion from the bounce until the end of the slow-roll inflationary phase in order to be consistent with the observations. However, the prediction for the duration of inflation in LQC depends on how the initial conditions for the dynamics are set.

In a previous work [30], it was investigated in details the duration of inflation for LQC models with monomial and Higgs-like potentials and which was considered initial conditions far in the contracting phase, thus well before the bounce (extending the analysis made in Refs. [10, 11, 24, 26, 33–38]). In the present paper, we have investigated the duration of inflation in these same models, including also the Starobinsky potential, but now from a different perspective concerning the initial conditions. As discussed, the dynamics in the LQC models considered here starts in the contracting phase sufficiently before the bounce, such that the kinetic energy of the inflaton field necessarily comes to dominate at the bounce. Then, we have shown that it is possible to estimate the inflaton field amplitude at some intermediate instant in the contracting phase, but still well before the bounce. With that value for the inflaton amplitude, we can forward the background dynamics up to the bounce instant and determine the value for the inflaton field at that instant,  $\phi_B$ . With  $\phi_B$  uniquely determined, all subsequent background dynamics from the bounce until the

---

slow-roll inflation for this kind of potentials in the presence of shear.

end of inflation can then be determined. In LQC models in which the evolution of the inflaton field is dominated by its kinetic energy at the quantum bounce, a slow-roll inflation phase is practically always reached as is also demonstrated by our results.

For all the models analyzed, we found that the number of  $e$ -folds of the pre-inflationary phase is approximately  $N_{\text{pre}} \sim 4$ . On the other hand, the number of inflationary  $e$ -folds changes considerably depending on the potential for the inflaton. Monomial potentials like  $V \propto |\phi|^5$  and with higher powers tend to predict a too small value for the number of inflationary  $e$ -folds and, thus, they are likely to be incompatible with the CMB data. The quartic potential,  $V \propto \phi^4$ , on the other hand, predicts the most likely  $N_{\text{infl}}$  to be around  $N_{\text{infl}} \sim 86$ , which suggests a very good possibility of leading to observable signatures from LQC in the spectrum of CMB data. For the quadratic model,  $V \propto \phi^2$ , the most likely  $N_{\text{infl}}$  is around  $N_{\text{infl}} \sim 147$ . This is in agreement with the results obtained in the earlier work done in Ref. [34]. With such high values of  $N_{\text{infl}}$  allowed by the quadratic potential, the effects from the quantum regime would probably be diluted to an unobservable level. For the Higgs-like symmetry-breaking potential we have shown that  $N_{\text{infl}}$  grows with the VEV  $v$  for the case of inflation occurring in the plateau (small-field) region. It reaches a maximum value for the number of  $e$ -folds at a VEV around  $v \sim 5m_{\text{Pl}}$  and beyond this value  $N_{\text{infl}}$  drops and tends to asymptote at around  $N_{\text{infl}} \sim 200$ . For inflation occurring in the large-field ( $|\phi| > |v|$ ) part of the potential  $N_{\text{infl}}$  has a weak dependence on  $v$ , being around  $N_{\text{infl}} \sim 110$  in the range of values of  $v$  we have considered. Even though these results were obtained for a Higgs-like potential, we expect the features displayed would also be present in other small field type of potentials, like hilltop and axion-like potentials. For the Starobinsky model, we predict a much higher value for  $N_{\text{infl}}$  when compared to the other potentials studied, with  $N_{\text{infl}} \sim 10^9$ . This implies in no potentially observable signal that could be searched for on CMB data as far as the Starobinsky model is considered in the context of LQC.

We have also shown in the present paper that the value of the Barbero-Immirzi parameter can affect strongly the constraints on the number of  $e$ -folds. The Barbero-Immirzi parameter is strictly a free parameter of the underlying LQG theory. Being related to the typical scale at the bounce, the Barbero-Immirzi parameter implies in different predictions for the power spectrum in LQC. In fact, what CMB actually constraints is the combination of the parameters  $\gamma$  and  $N_{\text{pre+infl}}$ , the total number of  $e$ -folds from the bounce until the end of inflation. Therefore, it is important to investigate the relation between the predictions for the number of  $e$ -folds in LQC with the value of  $\gamma$ . This analysis is performed in details, for the first time, in the present paper.

The results presented in this paper show that for different values of  $\gamma$  the predictions for the duration of inflation in LQC are considerably different. For the monomial po-

tentials, the predicted number of  $e$ -folds decreases with the value of  $\gamma$ . In particular it is interesting to see that, for example in the case of the sextic potential in LQC, although for the usual value of the Barbero-Immirzi parameter the model is in strong tension with the observations, for smaller values of the parameter, like  $\gamma \lesssim 0.1$ , it can be consistent with the increase of the predicted number of  $e$ -folds when  $\gamma$  is lower than the usual value adopted for it in the literature. For the Higgs-like potential, we have obtained that the number of  $e$ -folds increases with  $\gamma$  in the small field case, up to some critical value, beyond which, with the increase of  $\gamma$ , it starts to decrease. For the the large field case, on the other hand, the number of  $e$ -folds always decreases when  $\gamma$  increases. For the Starobinsky model we have obtained that the prediction for the number of  $e$ -folds decreases with  $\gamma$ . The number of  $e$ -folds can reach the limiting value of  $N \simeq 81$  for the value of the Barbero-Immirzi parameter  $\gamma \sim 1000$ , which is, nevertheless, a quite high value to be acceptable by the underlying LQG theory.

We conclude that the observable predictions in LQC models are dependent on the way initial conditions are set and also on the value of the Barbero-Immirzi parameter, being quite sensitive to the latter. Since the consistency of the models with the current data depends strongly on the value of this parameter, this paper highlights for the first time the importance of a careful analysis of the role of the Barbero-Immirzi parameter in LQC. Finally, in this paper we have analyzed only the case of a Universe with energy density made essentially of the inflaton field. As possible follow-ups of this paper, it would be interesting to perform a similar analysis when other energy contents are present, like from sources of anisotropies [35, 37] or when radiation is also present, which itself has been shown to lead to interesting results in the context of LQC [29, 30, 51, 62–65].

## VII. ACKNOWLEDGEMENTS

L.N.B. acknowledge financial support of the Coordenação de Aperfeiçoamento de Pessoal de Nível Superior (CAPES) - Finance Code 001. G.L.L.W.L. acknowledge financial support of the Conselho Nacional de Desenvolvimento Científico e Tecnológico (CNPq). L.L.G is supported by CNPq, under the Grant No. 307052/2019-2, and by the Fundação Carlos Chagas Filho de Amparo à Pesquisa do Estado do Rio de Janeiro (FAPERJ), Grant No. E-26/201.297/2021. R.O.R. is partially supported by research grants from CNPq, Grant No. 307286/2021-5, and from FAPERJ, Grant No. E-26/201.150/2021. One of us (L.L.G.) wishes to thank the Kavli Institute for the Physics and Mathematics of the Universe (IPMU) for kind hospitality.

### Appendix A: Obtaining $V_0$ through the CMB spectrum

Let us now briefly review the derivation of the normalization  $V_0$  for each of the potentials we have considered in this paper. The primordial scalar curvature power spectrum  $\Delta_{\mathcal{R}}$  is given by the standard expression [53]

$$\Delta_{\mathcal{R}} = \left( \frac{H_*^2}{2\pi\dot{\phi}_*} \right)^2, \quad (\text{A1})$$

where a subindex  $*$  means that the quantities are evaluated at the Hubble radius crossing  $k_*$  ( $k_* = a_* H_*$ ). This is typically assumed to happen around  $N_* \sim 50 - 60$  e-folds before the end of inflation. In this work we have assumed the fiducial value of 60 e-folds for illustration purposes. The value of  $V_0$  is fixed by the normalization of the primordial scalar of curvature power spectrum. The Planck Collaboration [61] gives for instance the value  $\ln(10^{10}\Delta_{\mathcal{R}}) \simeq 3.047$  (TT,TE,EE-lowE+lensing+BAO 68% limits). This is the value we have adopted in this paper to obtain the normalization  $V_0$ .

During the slow-roll regime of inflation, we can make the approximations  $H^2 \simeq 8\pi V/(3m_{\text{Pl}}^2)$  and  $\dot{\phi} \simeq -V_{,\phi}/(3H)$ . Thus,

$$\Delta_{\mathcal{R}} \simeq \frac{128\pi}{3m_{\text{Pl}}^6} \frac{V_*^3}{V_{,\phi_*}^2}, \quad (\text{A2})$$

for any given potential.

For the monomial power-law potentials Eq. (2.6), the Eq. (A2) gives

$$\Delta_{\mathcal{R}} = \frac{4}{3(4\pi)^n} \frac{1}{n^3} \frac{V_0^{\text{mon}}}{m_{\text{Pl}}^4} [n(2N_* + n)]^{n+1}, \quad (\text{A3})$$

where we have used that

$$\phi_* \equiv \phi(N_*) = \sqrt{(nm_{\text{Pl}}^2/4\pi)(2N_* + n)}. \quad (\text{A4})$$

Therefore, the normalization  $V_0$  obtained from CMB measurements gives

$$\frac{V_0^{\text{mon}}}{m_{\text{Pl}}^4} = \frac{3(4\pi)^n}{4} \frac{n^3}{[n(2N_* + n)]^{n+1}} \Delta_{\mathcal{R}}. \quad (\text{A5})$$

For the Higgs-like potential (2.7), we find, analogously, that

$$\Delta_{\mathcal{R}} = \frac{2\pi}{3m_{\text{Pl}}^6} \frac{V_0^{\text{Higgs}}}{m_{\text{Pl}}^4} \frac{(\phi_*^2 - v^2)^4}{\phi_*^2}. \quad (\text{A6})$$

Solving for  $V_0$ , we find

$$\frac{V_0^{\text{Higgs}}}{m_{\text{Pl}}^4} = \frac{3m_{\text{Pl}}^6}{2\pi} \Delta_{\mathcal{R}} \frac{\phi^2(N_*)}{[\phi_*^2(N_*) - v^2]^4}, \quad (\text{A7})$$

where  $\phi(N_*)$  is obtained from the expression (3.24), which gives two possible solutions,

$$\phi^2(N_*) = -v^2 W_0 \left[ -\frac{\phi_{\text{end}}^2}{v^2} \left( e^{\frac{N_*}{\pi} + \frac{\phi_{\text{end}}^2}{m_{\text{Pl}}^2}} \right)^{-\frac{m_{\text{Pl}}^2}{v^2}} \right], \quad (\text{A8})$$

and

$$\phi^2(N_*) = -v^2 W_{-1} \left[ -\frac{\phi_{\text{end}}^2}{v^2} \left( e^{\frac{N_*}{\pi} + \frac{\phi_{\text{end}}^2}{m_{\text{Pl}}^2}} \right)^{-\frac{m_{\text{Pl}}^2}{v^2}} \right], \quad (\text{A9})$$

where  $W_0$  and  $W_{-1}$  correspond to the Lambert functions and  $\phi_{\text{end}}$  is given by Eq. (3.25). It can be verified that the solution given by Eq. (A8) applies when inflation happens in the small field region of the potential, i.e., around the plateau region,  $|\phi| < |v|$ . The second solution given by Eq. (A9), on the other hand, applies in the large field region of the potential, i.e., when  $|\phi| > |v|$ .

For the Starobinsky potential, Eq. (2.8), the normalization  $V_0$  is found to be

$$\frac{V_0^{\text{Staro}}}{m_{\text{Pl}}^4} = \frac{e^{-8\sqrt{\frac{\pi}{3}}\frac{\phi_*}{m_{\text{Pl}}}}}{2\left(1 - e^{-4\sqrt{\frac{\pi}{3}}\frac{\phi_*}{m_{\text{Pl}}}}\right)^4} \Delta_{\mathcal{R}}, \quad (\text{A10})$$

where  $\phi_*$  is given by

$$\phi(N_*) = -\frac{m_{\text{Pl}}}{4\sqrt{3}\pi} \left\{ 4N_* + 3 + 2\sqrt{3} + \ln\left(-135 + 78\sqrt{3}\right) + 3W_{-1} \left[ -\left(1 + \frac{2}{\sqrt{3}}\right) e^{-\frac{4N_*}{3} - 1 - \frac{2}{\sqrt{3}}} \right] \right\}. \quad (\text{A11})$$

- 
- [1] A. D. Linde, Inflationary Cosmology, Lect. Notes Phys. **738**, 1-54 (2008) doi:10.1007/978-3-540-74353-8\_1 [arXiv:0705.0164 [hep-th]].  
 [2] J. A. Vázquez, L. E. Padilla and T. Matos, Inflationary Cosmology: From Theory to Observations,

- doi:10.31349/RevMexFisE.17.73 [arXiv:1810.09934 [astro-ph.CO]].  
 [3] L. Kofman, A. D. Linde and V. F. Mukhanov, Inflationary theory and alternative cosmology, JHEP **10**, 057 (2002) doi:10.1088/1126-6708/2002/10/057 [arXiv:hep-



- th/0206088 [hep-th].
- [4] Y. Akrami *et al.* [Planck], Planck 2018 results. X. Constraints on inflation, *Astron. Astrophys.* **641**, A10 (2020) doi:10.1051/0004-6361/201833887 [arXiv:1807.06211 [astro-ph.CO]].
- [5] A. Borde and A. Vilenkin, Eternal inflation and the initial singularity, *Phys. Rev. Lett.* **72**, 3305-3309 (1994) doi:10.1103/PhysRevLett.72.3305 [arXiv:gr-qc/9312022 [gr-qc]].
- [6] A. Borde, A. H. Guth and A. Vilenkin, Inflationary space-times are incomplete in past directions, *Phys. Rev. Lett.* **90**, 151301 (2003) doi:10.1103/PhysRevLett.90.151301 [arXiv:gr-qc/0110012 [gr-qc]].
- [7] J. Martin, C. Ringeval and V. Vennin, Encyclopædia Inflationaris, *Phys. Dark Univ.* **5-6**, 75-235 (2014) doi:10.1016/j.dark.2014.01.003 [arXiv:1303.3787 [astro-ph.CO]].
- [8] R. Brandenberger and X. m. Zhang, The Trans-Planckian Problem for Inflationary Cosmology Revisited, [arXiv:0903.2065 [hep-th]].
- [9] R. H. Brandenberger and J. Martin, Trans-Planckian Issues for Inflationary Cosmology, *Class. Quant. Grav.* **30**, 113001 (2013) doi:10.1088/0264-9381/30/11/113001 [arXiv:1211.6753 [astro-ph.CO]].
- [10] T. Zhu, A. Wang, G. Cleaver, K. Kirsten and Q. Sheng, Pre-inflationary universe in loop quantum cosmology, *Phys. Rev. D* **96**, no.8, 083520 (2017) doi:10.1103/PhysRevD.96.083520 [arXiv:1705.07544 [gr-qc]].
- [11] M. Shahalam, M. Sharma, Q. Wu and A. Wang, Preinflationary dynamics in loop quantum cosmology: Power-law potentials, *Phys. Rev. D* **96**, no.12, 123533 (2017) doi:10.1103/PhysRevD.96.123533 [arXiv:1710.09845 [gr-qc]].
- [12] M. Shahalam, K. Yesmakhanova and Z. Umurzakhova, Initial conditions of pre-inflation with Hilltop potential in loop quantum cosmology, [arXiv:2108.06218 [gr-qc]].
- [13] M. Martín-Benito, R. B. Neves and J. Olmedo, States of Low Energy in bouncing inflationary scenarios in Loop Quantum Cosmology, *Phys. Rev. D* **103**, 123524 (2021) doi:10.1103/PhysRevD.103.123524 [arXiv:2104.03035 [gr-qc]].
- [14] A. Ashtekar and P. Singh, Loop Quantum Cosmology: A Status Report, *Class. Quant. Grav.* **28**, 213001 (2011) doi:10.1088/0264-9381/28/21/213001 [arXiv:1108.0893 [gr-qc]].
- [15] A. Barrau, T. Cailleteau, J. Grain and J. Mielczarek, Observational issues in loop quantum cosmology, *Class. Quant. Grav.* **31**, 053001 (2014) doi:10.1088/0264-9381/31/5/053001 [arXiv:1309.6896 [gr-qc]].
- [16] I. Agullo and P. Singh, Loop Quantum Cosmology, doi:10.1142/9789813220003\_0007 [arXiv:1612.01236 [gr-qc]].
- [17] M. Bojowald, Loop quantum cosmology, *Living Rev. Rel.* **8**, 11 (2005) doi:10.12942/lrr-2005-11 [arXiv:gr-qc/0601085 [gr-qc]].
- [18] A. Ashtekar, M. Bojowald and J. Lewandowski, Mathematical structure of loop quantum cosmology, *Adv. Theor. Math. Phys.* **7**, no.2, 233-268 (2003) doi:10.4310/ATMP.2003.v7.n2.a2 [arXiv:gr-qc/0304074 [gr-qc]].
- [19] A. Ashtekar, T. Pawłowski and P. Singh, Quantum nature of the big bang, *Phys. Rev. Lett.* **96**, 141301 (2006) doi:10.1103/PhysRevLett.96.141301 [arXiv:gr-qc/0602086 [gr-qc]].
- [20] A. Ashtekar and D. Sloan, Loop quantum cosmology and slow roll inflation, *Phys. Lett. B* **694**, 108-112 (2011) doi:10.1016/j.physletb.2010.09.058 [arXiv:0912.4093 [gr-qc]].
- [21] B. Elizaga Navascués and G. A. M. Marugán, Hybrid Loop Quantum Cosmology: An Overview, *Front. Astron. Space Sci.* **8**, 81 (2021) doi:10.3389/fspas.2021.624824 [arXiv:2011.04559 [gr-qc]].
- [22] K. Banerjee, G. Calcagni and M. Martín-Benito, Introduction to loop quantum cosmology, *SIGMA* **8**, 016 (2012) doi:10.3842/SIGMA.2012.016 [arXiv:1109.6801 [gr-qc]].
- [23] B. F. Li, P. Singh and A. Wang, Qualitative dynamics and inflationary attractors in loop cosmology, *Phys. Rev. D* **98**, no.6, 066016 (2018) doi:10.1103/PhysRevD.98.066016 [arXiv:1807.05236 [gr-qc]].
- [24] M. Sharma, M. Shahalam, Q. Wu and A. Wang, Preinflationary dynamics in loop quantum cosmology: Monodromy Potential, *JCAP* **11**, 003 (2018) doi:10.1088/1475-7516/2018/11/003 [arXiv:1808.05134 [gr-qc]].
- [25] B. F. Li, P. Singh and A. Wang, Genericness of pre-inflationary dynamics and probability of the desired slow-roll inflation in modified loop quantum cosmologies, *Phys. Rev. D* **100**, no.6, 063513 (2019) doi:10.1103/PhysRevD.100.063513 [arXiv:1906.01001 [gr-qc]].
- [26] M. Shahalam, M. Al Ajmi, R. Myrzakulov and A. Wang, Revisiting pre-inflationary Universe of family of  $\alpha$ -attractor in loop quantum cosmology, *Class. Quant. Grav.* **37**, no.19, 195026 (2020) doi:10.1088/1361-6382/aba486 [arXiv:1912.00616 [gr-qc]].
- [27] A. Barrau, A pure general relativistic non-singular bouncing origin for the Universe, *Eur. Phys. J. C* **80**, no.6, 579 (2020) doi:10.1140/epjc/s10052-020-8158-5 [arXiv:2005.04693 [gr-qc]].
- [28] S. Bedić and G. Vereshchagin, Probability of inflation in Loop Quantum Cosmology, *Phys. Rev. D* **99**, no.4, 043512 (2019) doi:10.1103/PhysRevD.99.043512 [arXiv:1807.06554 [gr-qc]].
- [29] L. L. Graef and R. O. Ramos, Probability of Warm Inflation in Loop Quantum Cosmology, *Phys. Rev. D* **98**, no.2, 023531 (2018) doi:10.1103/PhysRevD.98.023531 [arXiv:1805.05985 [gr-qc]].
- [30] L. N. Barboza, L. L. Graef and R. O. Ramos, Warm bounce in loop quantum cosmology and the prediction for the duration of inflation, *Phys. Rev. D* **102**, no.10, 103521 (2020) doi:10.1103/PhysRevD.102.103521 [arXiv:2009.13587 [gr-qc]].
- [31] A. H. Guth, The Inflationary Universe: A Possible Solution to the Horizon and Flatness Problems, *Phys. Rev. D* **23**, 347-356 (1981) doi:10.1103/PhysRevD.23.347
- [32] I. Agullo, A. Ashtekar and W. Nelson, The pre-inflationary dynamics of loop quantum cosmology: Confronting quantum gravity with observations, *Class. Quant. Grav.* **30**, 085014 (2013) doi:10.1088/0264-9381/30/8/085014 [arXiv:1302.0254 [gr-qc]].
- [33] A. Ashtekar and D. Sloan, Probability of Inflation in Loop Quantum Cosmology, *Gen. Rel. Grav.* **43**, 3619-3655 (2011) doi:10.1007/s10714-011-1246-y [arXiv:1103.2475 [gr-qc]].

- [34] L. Linsefors and A. Barrau, Duration of inflation and conditions at the bounce as a prediction of effective isotropic loop quantum cosmology, *Phys. Rev. D* **87**, no.12, 123509 (2013) doi:10.1103/PhysRevD.87.123509 [arXiv:1301.1264 [gr-qc]].
- [35] L. Linsefors and A. Barrau, Exhaustive investigation of the duration of inflation in effective anisotropic loop quantum cosmology, *Class. Quant. Grav.* **32**, no.3, 035010 (2015) doi:10.1088/0264-9381/32/3/035010 [arXiv:1405.1753 [gr-qc]].
- [36] B. Bolliet, A. Barrau, K. Martineau and F. Moulin, Some Clarifications on the Duration of Inflation in Loop Quantum Cosmology, *Class. Quant. Grav.* **34**, no.14, 145003 (2017) doi:10.1088/1361-6382/aa7779 [arXiv:1701.02282 [gr-qc]].
- [37] K. Martineau, A. Barrau and S. Schander, Detailed investigation of the duration of inflation in loop quantum cosmology for a Bianchi-I universe with different inflaton potentials and initial conditions, *Phys. Rev. D* **95**, no.8, 083507 (2017) doi:10.1103/PhysRevD.95.083507 [arXiv:1701.02703 [gr-qc]].
- [38] L. Chen and J. Y. Zhu, Loop quantum cosmology: The horizon problem and the probability of inflation, *Phys. Rev. D* **92**, no.8, 084063 (2015) doi:10.1103/PhysRevD.92.084063 [arXiv:1510.03135 [gr-qc]].
- [39] A. Barrau, K. Martineau and F. Moulin, A status report on the phenomenology of black holes in loop quantum gravity: Evaporation, tunneling to white holes, dark matter and gravitational waves, *Universe* **4**, no.10, 102 (2018) doi:10.3390/universe4100102 [arXiv:1808.08857 [gr-qc]].
- [40] J. Armas and J. Armas, Conversations on Quantum Gravity, doi:10.1017/9781316717639
- [41] S. K. Asante, B. Dittrich and H. M. Haggard, Effective Spin Foam Models for Four-Dimensional Quantum Gravity, *Phys. Rev. Lett.* **125**, no.23, 231301 (2020) doi:10.1103/PhysRevLett.125.231301 [arXiv:2004.07013 [gr-qc]].
- [42] S. K. Asante, B. Dittrich and J. Padua-Arguelles, Effective spin foam models for Lorentzian quantum gravity, *Class. Quant. Grav.* **38**, no.19, 195002 (2021) doi:10.1088/1361-6382/ac1b44 [arXiv:2104.00485 [gr-qc]].
- [43] L. Perlov, Barbero-Immirzi value from experiment, *Mod. Phys. Lett. A* **36**, no.27, 2150192 (2021) doi:10.1142/S0217732321501923 [arXiv:2005.14141 [gr-qc]].
- [44] B. Broda and M. Szanecki, A relation between the Barbero-Immirzi parameter and the standard model, *Phys. Lett. B* **690**, 87-89 (2010) doi:10.1016/j.physletb.2010.05.004 [arXiv:1002.3041 [gr-qc]].
- [45] S. Mercuri and V. Taveras, Interaction of the Barbero-Immirzi Field with Matter and Pseudo-Scalar Perturbations, *Phys. Rev. D* **80**, 104007 (2009) doi:10.1103/PhysRevD.80.104007 [arXiv:0903.4407 [gr-qc]].
- [46] S. J. Gates, Jr., S. V. Ketov and N. Yunes, Seeking the Loop Quantum Gravity Barbero-Immirzi Parameter and Field in 4D,  $N = 1$  Supergravity, *Phys. Rev. D* **80**, 065003 (2009) doi:10.1103/PhysRevD.80.065003 [arXiv:0906.4978 [hep-th]].
- [47] S. Boudet, The Immirzi field in modified gravity: super-entropic black holes with scalar hair, [arXiv:2203.08558 [gr-qc]].
- [48] C. Pigozzo, F. S. Bacelar and S. Carneiro, On the value of the Immirzi parameter and the horizon entropy, *Class. Quant. Grav.* **38**, no.4, 045001 (2021) doi:10.1088/1361-6382/abce6a [arXiv:2001.03440 [gr-qc]].
- [49] S. Carneiro and C. Pigozzo, Quasinormal modes and horizon area quantisation in Loop Quantum Gravity, *Gen. Rel. Grav.* **54**, 20 (2022) [erratum: *Gen. Rel. Grav.* **54**, no.3, 25 (2022)] doi:10.1007/s10714-022-02910-x [arXiv:2012.00227 [gr-qc]].
- [50] P. J. Wong, Implementation of conformal scaling in loop quantum gravity via the Barbero-Immirzi parameter, doi:10.1142/9789813226609\_0520
- [51] M. Benetti, L. Graef and R. O. Ramos, Observational Constraints on Warm Inflation in Loop Quantum Cosmology, *JCAP* **10**, 066 (2019) doi:10.1088/1475-7516/2019/10/066 [arXiv:1907.03633 [astro-ph.CO]].
- [52] K. A. Meissner, Black hole entropy in loop quantum gravity, *Class. Quant. Grav.* **21**, 5245-5252 (2004) doi:10.1088/0264-9381/21/22/015 [arXiv:gr-qc/0407052 [gr-qc]].
- [53] D. H. Lyth and A. R. Liddle, *The primordial density perturbation: Cosmology, inflation and the origin of structure*, (Cambridge University Press, Cambridge, 2009).
- [54] P. A. R. Ade *et al.* [BICEP and Keck], Improved Constraints on Primordial Gravitational Waves using Planck, WMAP, and BICEP/Keck Observations through the 2018 Observing Season, *Phys. Rev. Lett.* **127**, no.15, 151301 (2021) doi:10.1103/PhysRevLett.127.151301 [arXiv:2110.00483 [astro-ph.CO]].
- [55] M. Benetti and R. O. Ramos, Warm inflation dissipative effects: predictions and constraints from the Planck data, *Phys. Rev. D* **95**, no.2, 023517 (2017) doi:10.1103/PhysRevD.95.023517 [arXiv:1610.08758 [astro-ph.CO]].
- [56] A. A. Starobinsky, A New Type of Isotropic Cosmological Models Without Singularity, *Phys. Lett. B* **91**, 99-102 (1980) doi:10.1016/0370-2693(80)90670-X
- [57] M. S. Turner, Coherent Scalar Field Oscillations in an Expanding Universe, *Phys. Rev. D* **28**, 1243 (1983) doi:10.1103/PhysRevD.28.1243
- [58] M. Bastero-Gil, A. Berera, R. Brandenberger, I. G. Moss, R. O. Ramos and J. G. Rosa, The role of fluctuation-dissipation dynamics in setting initial conditions for inflation, *JCAP* **01**, 002 (2018) doi:10.1088/1475-7516/2018/01/002 [arXiv:1612.04726 [astro-ph.CO]].
- [59] M. Cicoli, C. P. Burgess and F. Quevedo, Fibre Inflation: Observable Gravity Waves from IIB String Compactifications, *JCAP* **03**, 013 (2009) doi:10.1088/1475-7516/2009/03/013 [arXiv:0808.0691 [hep-th]].
- [60] J. B. Munoz and M. Kamionkowski, Equation-of-State Parameter for Reheating, *Phys. Rev. D* **91**, no.4, 043521 (2015) doi:10.1103/PhysRevD.91.043521 [arXiv:1412.0656 [astro-ph.CO]].
- [61] N. Aghanim *et al.* [Planck], Planck 2018 results. VI. Cosmological parameters, *Astron. Astrophys.* **641**, A6 (2020) [erratum: *Astron. Astrophys.* **652**, C4 (2021)] doi:10.1051/0004-6361/201833910 [arXiv:1807.06209 [astro-ph.CO]].
- [62] R. Herrera, Warm inflationary model in loop quantum cosmology, *Phys. Rev. D* **81**, 123511 (2010) doi:10.1103/PhysRevD.81.123511 [arXiv:1006.1299 [astro-ph.CO]].
- [63] K. Xiao and J. Y. Zhu, A Phenomenology analysis of

- the tachyon warm inflation in loop quantum cosmology, Phys. Lett. B **699**, 217 (2011).
- [64] X. M. Zhang and J. Y. Zhu, Warm inflation in loop quantum cosmology: a model with a general dissipative coefficient, Phys. Rev. D **87**, no. 4, 043522 (2013).
- [65] K. Xiao and S. Q. Wang, Pre-inflation dynamical behavior of warm inflation in loop quantum cosmology, Mod. Phys. Lett. A **35**, no.35, 2050293 (2020) doi:10.1142/S0217732320502934